Israel Oceanographic & Limnological Research Ltd
Yigal Allon Kinneret Limnological Laboratory
P.O.Box 447, Migdal 14950, Israel
Tel: 972 4 6721444; Fax: 972 4 6724627; www.ocean.org.il e-mail: kll@ocean.org.il

חקר ימים ואגמים לישראל בע"מ
המעבדה לחקר הכנרת ע"ש יגאל אלון
ת.ד. 447, מיגדל 14950

Spatial distribution of the bloom-forming dinoflagellate *Peridinium gatunense* in Lake Kinneret

The Yigal Allon Kinneret Limnological Laboratory
Winter-Spring 2007 experiment

Internal Report

Edited by
Assaf Sukenik

Contributors: Gal G., Eckert W., Hadas O., Nishri, A, Ostrovsky I., Parparov A., Rimer A., Shilo E., Tibor G., Wynne D., Yacobi Y.Z., Zohary T.

IOLR Report T3/2008

March 2008

Acknowledgment

This report is the outcome of a concentrated effort of the staff of the Yigal Allon Kinneret Limnological Laboratory (IOLR). The devotion and industriousness of our colleagues made this experiment possible. We wish to express our special thanks to the boat skippers: Meir Hatab, Moti Diamant and Boaz Avraham and to the field and laboratory technicians: Semion Kaganovsky, Uri Lachinsky, Mina Bizitch, Ehud Wagner, Shimshon Zakai, Edit Leibovitch, Beni Sulimani, Riki Pinkas, Sara Chava, Nir Koren, Nehama Malinsky-Rushansky, Yehudit Viner-Motzini. Special thanks also to Miki Schlichter, KLL information technologist and the office staff Yochi Kachila and Gil Ferster.

Spatial distribution of the bloom-forming dinoflagellate *Peridinium gatunense* in Lake Kinneret

Executive Summary

In Lake Kinneret, the dinoflagellate *Peridinium gatunense* forms spring blooms of intensities comparable to those of red tides. These blooms are characterized by distinct spatial heterogeneity or patchiness, as well as diurnal vertical migration of the population. Horizontally, *Peridinium* is typically distributed in patches scaling hundreds of meters to several km, visible from shore as coffee-brown regions within the bluer surrounding water. *Peridinium* cell densities inside a patch usually exceed 1000 cells/mL (ca 300 mg chlorophyll m^{-3}), whereas outside the patch the concentrations are typically one or two orders of magnitude lower.

The main goal of this study was to characterize the patchy nature of Peridinium blooms in Lake Kinneret and to identify and quantify the physical and/or biological processes that control this patchy nature.

In a coordinated and concentrated effort we studied the spatial distribution and dynamic variations of *Peridinium* population in the northern area of Lake Kinneret for three consecutive days during the last week of March 2007. The sampling approach that was practiced in this study was based on a predetermined sampling grid of known dimensions and precise location. The location of the grid was chosen based on initial information collected at a larger area were *Peridinium* patches were observed.

It was clearly demonstrated that *Peridinium* patches migrated across the sampling grid and the data collected during several consecutive sampling campaigns represented inside and outside the patch conditions. In some cases, large portion of the patch were sampled whereas in other cases only the edges of a patch were sampled.

Since the location of the experiment was at a close vicinity to the entrance of Jordan River to Lake Kinneret, a site which is characterized by a supply of nutrients and other growth factors, it was expected that the emerging *Peridinium* population will maintain high growth rate as long as its location is restricted to the Jordan River inlet area.

The collected data suggest high correlation between the size of the *Peridinium* population (in terms of chlorophyll concentration) and the ratio of Jordan River water (traced by low salinity, low chloride and high nitrate concentrations) in the studied location. Satellite images and earlier studies indicated that the *Peridinium* patches exist mainly in the northern part of the lake where Jordan River enters the lake. Therefore, this area is proposed as the site of population development and growth. Such a growth is supported by nutrients and chemical conditions provided by the river inflow. The distribution of the developed *Peridinium* population to other locations in Lake Kinneret is facilitated as the population "tracks" the Jordan River plume in Lake Kinneret.

Based on the data collected in this study we postulate that a bulk of water enriched with *Peridinium* population is disintegrated from the "hatching" and "nursing" area (Jordan River inlet area) and starts its migration in the lake in accordance with the physical and hydrodynamic forces.

The *Peridinium* population continues to take advantage of the relatively nutrient enriched confined pocket, and use it for further duplications. It is important to note that *Peridinium* duplication can be maintained for one or tow divisions even when the nutrient diminished due to its wide range of nutrient yields.

High density *Peridinium* patches were accompanied by dense population of microzooplankton and herbivorous zooplankton species whereas predatory zooplankton species were preferentially located outside the patch. Gross calculations of the nutrient release rate by zooplankton inside the patch indicate that they could provide variable amount of the P needs by the *Peridinium* via nutrient recycling.

The patch migration continues along the "Jordan River" trail in Lake Kinneret, from the north area, the site of the population emergence, along the northwest cost and to the lake center, in accordance with the results of the circulation simulations model ROMS for the dispersion of an inert tracer in Lake Kinneret. Since the *Peridinium* patch is definitely not an inert tracer, its signal increases during the migration process.

Based on this model, it is expected that a single patch migrating in the lake is of different age or developmental stage then another patch. Furthermore, a migrating patch can be a source of additional secondary patch which can be disintegrated from the main patch due to temporary wind gusts and local currents. Such an event is most likely to occur as the *Peridinium* population is concentrated as a thin layer at the upper part of the water column, a phenomenon known as diurnal vertical migration – DVM.

Table of contents

Spatial distribution of the bloom-forming dinoflagellate *Peridinium gatunense* in Lake Kinneret

The phenomenon

In Lake Kinneret, the dinoflagellate *Peridinium gatunense* forms spring blooms of intensities comparable to those of red tides. These blooms are characterized by distinct spatial heterogeneity or patchiness, as well as diurnal vertical migration of the population. Horizontally, *Peridinium* is typically distributed in patches scaling hundreds of meters to several km, visible from shore as coffee-brown regions within the bluer surrounding water. *Peridinium* cell densities inside a patch usually exceed 1000 cells/mL (ca 300 mg chlorophyll m^{-3}), whereas outside the patch the concentrations are typically one or two orders of magnitude lower.

Examples of the typically heterogeneous spatial distribution of *Peridinium* in Lake Kinneret are presented in Figure 1 as maps of chlorophyll concentrations at the depth of maximum chlorophyll, based on a series of surveys conducted during the spring of 2003.
Patches of high chlorophyll were located at different zones of the lake. During the morning, dense patches of *peridinium* were characterized by a relatively thin layer (1-2 m) of high chlorophyll density up to 350 mg m^{-3}, located near the water surface. The observed *peridinium* patches were almost at basin-scale size i.e. 20-50 square kilometers in area. The fact that the *peridinium* patches were found in Lake Kinneret at the center of the lake and were not restricted to the northern sublittoral zone near the source of fresh nutrients i.e. the inlet of Jordan River, suggests the effect of physical processes in the formation of the observed patchy pattern.

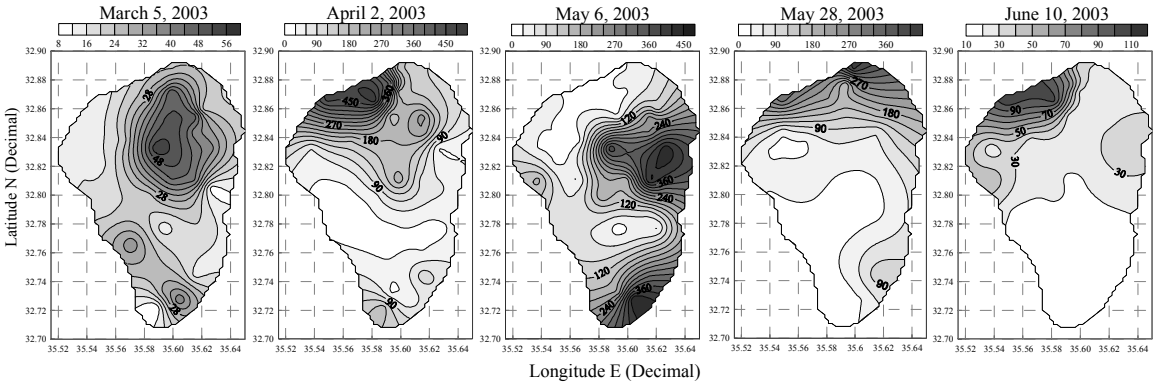

Figure 1: The spatial distribution of chlorophyll *a* in Lake Kinneret, at the depth of maximum phytoplankton concentration, measured on various dates during the 2003 bloom of *Peridinium gatunense* in Lake Kinneret. Chlorophyll maximum values ranged between 50 mg m^{-3} and 500 mg m^{-3} as the bloom developed between March 5 and May 6.

Additional factor possibly involved in this spatial heterogeneity is the diel migration of the *Peridinium* population. During calm and sunny mornings, *Peridinium* form a prominent biomass peak within the uppermost 1-2 m layer. Between midnight and sunrise, however, no aggregation is visible and *Peridinium* is evenly distributed over the water column. As the bloom progresses the bloom peak appeared deeper in the water column, between 2-4 m before noon and at 5-7 m in the afternoon, suggesting that *Peridinium* aggregate at the depth of optimal light intensity. During storms, however, *Peridinium* cannot maintain its preferred position in the water column, resulting in a homogeneous vertical distribution. Several biotic and abiotic factors were thought

to affect the diel vertical migration, including active movement towards the layer with optimum light intensity (during the light hours) or temperature, settling during the night to depths of higher nutrient concentrations, and wind created shear mixing (dominant in the evenings) that vertically disperses the accumulated population.

Objectives of the study

The main goal of the study was to characterize the patchy nature of *Peridinium* blooms in Lake Kinneret and to identify and quantify the physical and/or biological processes that control this patchy nature.

Working hypotheses

1. The 3D distribution of the *Peridinium* population in a lacustrine environment is governed by a concerted vertical migration of the population and horizontal dispersion by lateral advection and mixing.
2. Active vertical migration of *Peridinium gatunense* in Lake Kinneret during a daily cycle is governed by abiotic factors (light, temperature, nutrients, water density gradient) and biotic factors (intra-population factor or quorum factor, but not grazing).
3. Horizontal dispersion is dominated by in-lake physical circulation and turbulent currents although biological factors such as growth and population chemical attraction cannot be excluded.

Conceptual model

Figure 2 presents a conceptual model of the biotic and abiotic factors that are presumably involved in the patchiness phenomenon of *Peridinium* in Lake Kinneret. The wind is considered as a major factor that drives the in-lake currents and the location of patches. Specific features of *Peridinium* cells such as motility, settling, nutrienent aqusition and nutrient cell quota are the biotic factors that may control the momentary position of individual cells and the whole population.

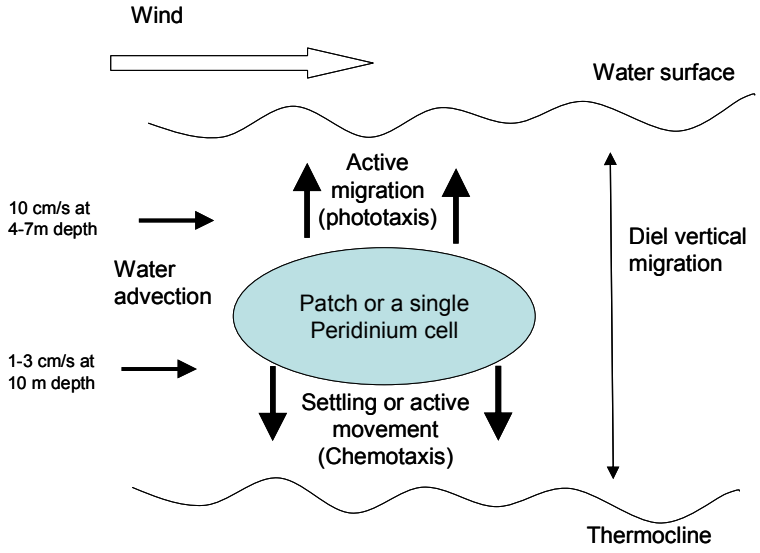

Figure 2: A conceptual model of the biotic and abiotic factors that are presumably involved in the patchiness phenomenon of the *Peridinium* bloom in Lake Kinneret.

Work plan and procedures

Location

In order to identify the physical, chemical and biological processes involved in patch formation and the dynamics of patch migration, several consecutive sampling campaigns were carried out during a 44 h period. The concept was to sample over time at fixed stations while patches of *Peridinium* pass through these stations. The field operation was restricted to an area of 3 by 2 km in the northwestern part of the lake (marked by a square in Fig. 3A) (Fig. 3B).

The geographic location of the grid and its actual dimensions were determined after conducting a preliminary FP survey 6 h prior to the beginning of the main field operation. The preliminary survey (T0) was used to better define the location of the sampling grid for the entire operation and it is presented in Figure 3C together with the location of the sampling grid. The structure of a small grid within a larger external grid was planned to cover patches of different sizes and resolution. The distribution of chlorophyll in the preliminary survey is presented in Figure 3C.

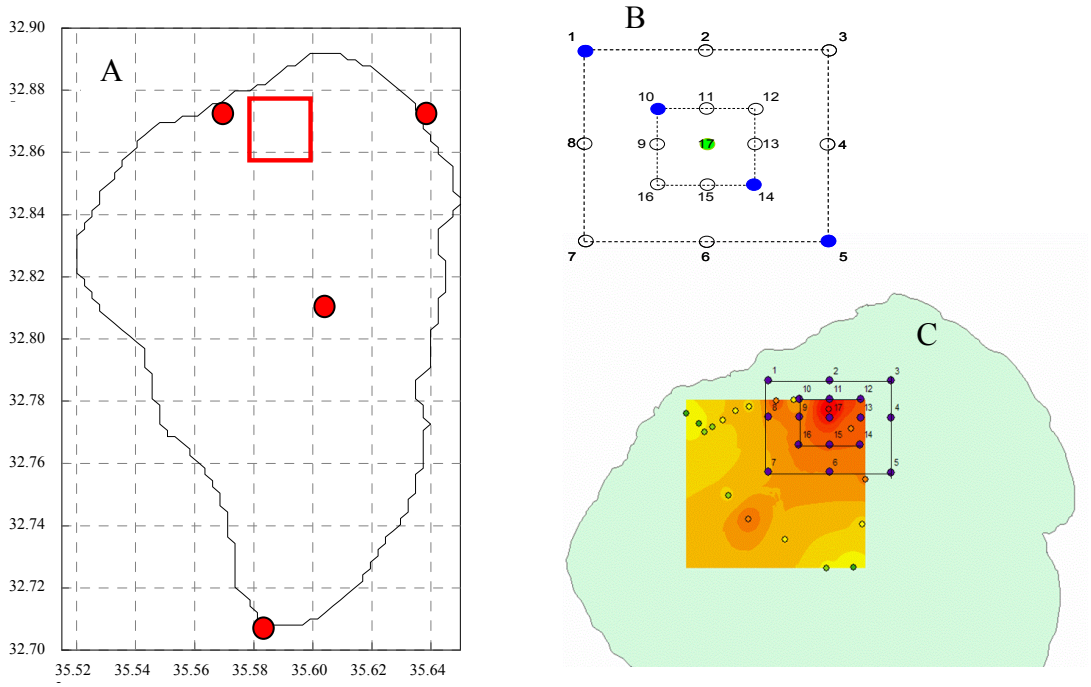

Figure 3: (A) Location of meteorological stations (large red dots) in Lake Kinneret and the sampling grid for the 2007 *Peridinium* operation (red sqare); (B) details of the sampling grid for the 2007 *Peridinium* operation. At stations marked by blue dots – water samples were collected at 1 and 7 m, green dots – water samples collected from multiple depths (0, 1, 2, 3, 5, 7, 10 and 15 m). At stations marked by open circles, blue dots & green dot – Fluoroprobe profiles and water sampling were taken from the depth of chlorophyll maximum; (C) the location of the sampling grid superimposed over the chlorophyll distribution map based on a preliminary Fluoroprobe (FB) survey carried out 6 h prior to the main operation.

Sampling schedule

Sampling was concentrated in a 44 h period, starting at 16:00 hr on 26 March and ending at 12:00 hr on 28 March, during which 7 campaigns were conducted, referred to in Table 1 as T1 to T7. Samples were collected from different locations according to the sampling grid presented in Figure 3B. Each sampling campaign was restricted to a 3-4 h period to allow the completion of the sampling tasks at all stations. Table 1 gives the timing of each sampling campaign and additional activities conducted concurrently.

Table 1: Timing and duration of the sampling campaigns conducted during the 2007 *Peridinium* operation in Lake Kinneret.

	Date	Sampling time	Comments and additional activities
T0	March 26, 2007	0810 - 1030	FP* preliminary survey
T1	March 26, 2007	1600 – 2045	U-TUMS** 1400 – 1530 at lt. 32.86E
T2	March 26, 2007	2300 – 0130	U-TUMS** 2345 – 0125 at lt. 32.84E
T3	March 27, 2007	0400 – 0700	
T4	March 27, 2007	1030 - 1400	
T5	March 27, 2007	1630 - 1930	U-TUMS** 2215 – 2350 at lt. 32.84E
T6	March 28, 2007	0000 - 0300	
T7	March 28, 2007	0800 - 1200	U-TUMS** 1345 – 1520 at lt. 32.84E

* FP - Fluoroprobe
** U-TUMS - underwater-towed undulating monitoring system

Models and simulations of water circulation

Simulations of atmospheric (RAMS, Regional Atmosphere Modeling System) and oceanic (ROMS, Regional Ocean Modeling System) general circulation models were run prior to the experiment to estimate the expected current field (velocity and directions) in the experimental region and at time intervals thereafter.

Mode of Operation

At each sampling campaign (T1 to T7) the boat visited the designated sampling stations and the water column was sampled by BBE-Fluoroprobe and fluorescence signal and temperature profiles were recorded. Light intensity in the water column was recorded during daytime using a LICOR light meter. Water samples (ca 1-5 liters) were collected from the chlorophyll maximum layer at each sampling station for cell counts and chlorophyll determination.

Water samples (ca 1-5 liters) were collected from stations 1, 5, 10 and 14 at 1 m and 7 m depth for further chemical and biological analyses.

Water samples (ca 1-5 liters) were collected from station 17 (the center of the sampling grid) at water depths of 0, 1, 2, 3, 5, 7, 10 and 15 m for further chemical and biological analyses.

The field survey was accompanied by continuous measurements of meteorological data at 4 stations around and within the lake (Figure 3A), and continuous measurements of currents conducted in Station A and near by the sampling grid. These data was the basis for calibrations and simulations of currents in the relevant area using state of the art atmospheric and oceanic general circulation models.

Analytical approach

Chemistry – the following parameters were measured in water samples collected at various sampling sites and at different sampling times: Total suspended solids (TSS), Particulate organic carbon (POC), and Particle size distribution. Oxygen, pH, Turbidity, SRP by Magic, total P, DIN species (NO_3, NO_2, NH_4), CHN content in particles (biomass).

Biology - the following parameters were measured in water samples collected at various sampling sites and at different sampling times: Phytoplankton – species composition and intra-species morphological variability (i.e. cell dimensions), Zooplankton species composition and abundance, Bacterial activity, Alkaline phosphatase activity, Fatty acid composition in biomass

U-TUMS operation

Spatial resolution of several *in situ* limnological parameters (temperature, turbidity, salinity, and chlorophyll) was recorded by an underwater-towed undulating monitoring system (U-TUMS). The U-TUMS is composed of a vehicle (carrier), a set of sensors, and navigation devices (geographic positioning system-GPS, SONAR, and speedometer) which are interconnected and operated via an on-board computer. The U-TUMS vehicle - MiniBAT (GuildLine Canada) is loaded with: (1) a multi-sensor probe CTD that measures water electric conductivity, temperature, and depth (Applied Microsystems Limited, Canada); (2) an optical backscatter sensor that measures water turbidity (OBS-3, D&A Instrument Company, USA), and (3) a fluorometer for sensing chlorophyll (MinitracaII, Chelsea Instrument, UK). The fast response of these sensors assures an accurate measurement at a distance resolution of less than 15 cm within the water column, while the vehicle is towed at a speed of 3-4 knots and undulates (diving or climbing) at rates of up to 50 cm s^{-1}. The on-board computer operates the vehicle's steering mechanism and causes the vehicle to undulate from near-surface to near-bottom (the maximum diving depth was restricted to 12 m. The computer also collects data from sensors and position information of the vehicle within the water body and presents it in real time. The collected data was then analyzed to produce a two-dimensional vertical view of the limnological parameters measured along the U-TUMS transect. During this study the U-TUMS was operated four times during the 36 hrs experimental period along a west to east and back transects on the same geographic latitude. The duration for each transect was ca 50 min, representing a survey of about 8 km.

SISCAL

SISCAL is a software package for processing satellite images and spectral data to estimate the distribution of various environmental parameters. SISCAL is integrated in the ArcGis software. Satellite images of Lake Kinneret area were acquired from MERIS RR satellite prior, during and after our study and processed by SISCAL. The relative distribution of chlorophyll in Lake Kinneret was calculated to reveal the presence and location of phytoplankton patches.

Results

The 2007 *Peridinium* operation represents a multidiciplinary effort aimed at characterizitation of the patchy nature of the *Peridinium* bloom and at elucidation of the physical and biological processes associated with the patchiness phenomenon. The result section is divided into several chapters, each of which summarizes the results obtained within a specific analytical discipline. The dynamics of the patchiness phenomenon is firstly described on a daily and weekly scale based on satellite images and in situ measurments by fluorescence and other fast responding electronic and optic devices. Then we provide detailed analysis of the patches structure and characterize their dynamics. Detailed studies were performed to identify short term variations in cell morphology and biochemical properties of the *Peridinium* population within, and outside a patch. Continuous measurments of wind performed at several stations on and around the lake were used to drive the general circulation model – ROMS to predict the current structure in the entire lake and in the study area.

1. Peridinium bloom event in Lake Kinneret as recorded by MERIS RR satellite and SISCAL application

In February 2007 a population of *Peridinium* was already observed in Lake Kinneret. Satellite images, collected and analyzed during February and early March 2007, clearly demonstrated the presence of distinct patches of chlorophyll which were attributed to the developed population of *Peridinium*. The satelitte images presented in Figure 4 suggest the migration of a chlorophyll enriched patch along the costal area. On March 4 a dense patch was observed at the north eastern area of the lake. Few weeks later the chlorophyll patch migrated westward along the shore line and further migrated to the southern end of lake.

Due to meteorological constrains, mainly clouds and poor visibility, satellite images are not available everyday. Furthermore, a satellite image is taken once a day as the satellite overcast our region, thereby a detailed analysis of the dynamics of patches is hindered and spatial variations on time scales shorter than 24 h are missed.

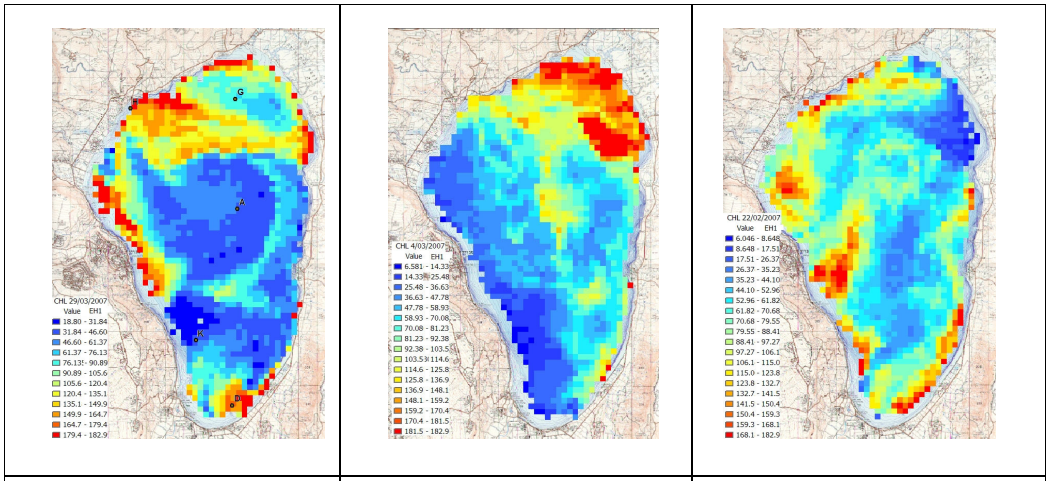

February 4, 2007	March 4, 2007	March 29, 2007

Figure 4: Chlorophyll distribution maps based on spectral data obtained from MERIS FR satellite on different dates and processed in SISCAL. Red color represents high chlorophyll concentration (ca 180 mg m^{-3}); blue color represents low chlorophyll concentration (range: 6 - 18 mg m^{-3}).

No SISCAL processed satellite images could be acquired during the 2007 *Peridinium* operation due to atmospheric conditions. Nevertheless, the spatial resolution of the MERIS FR satellite is 300 m by 300 m which provide relatively good definition of the patch contours and boundaries. The data collected before the operation, during February - March 2007 (Fig. 4) clearly demonstrated heterogeneous distribution of chlorophyll in Lake Kinneret .

2. *Spatial and temporal distribution of Peridinium biomass*

Two analytical devices were operated to follow the spatial and temporal distribution *Peridinium*: (a) The Fluoroprobe (FB) manufectured by BBE- Moldenka that was operated as a profiler to estimate the chlorophyll concentration and the the structure of the phytoplankton community based on their pigment suit. Data collected at various locations within the sampling grid were integrated into discrete chlorophyll depth profiles or interpolated maps of chlorophyll concentration within the sampling grid. (b) The U-TUMS was operated four times during the 44 hrs experimental period along a East-West transects on the same geographic latitude. The first U-TUMS survey was conducted just before the initiation of 2007 *Peridinium* operation along latitude line 32.862 E whereas the three other surveys were operated ~2 km further south along latitude 32.84 E (Table 1). The fluorescence and the turbidity data were integrated to produce iso-lines and depth concentration maps along the survey transects.

1. The Fluroprobe data - horizontal and vertical distribution (Yosef Yacobi, Assaf Sukenik, Ilia Ostrovsky)

Spatial distribution maps of chlorophyll concentration at 1 m depth are presented in Figure 5 for 8 consequtive data acquisition campigns. The exact location of the studied area is presented in Figure 3C. Note that at T0 only part of the studied grid was covered while using arbitrary sampling locations.

All the chlorophyll distribution maps shown in Figure 5 are drawn to the same color scale, ranging 25 to 700 mg chl m^{-3}. The ca 6 hours intervals between data acquisition campaigns clearly indicated that the horizontal movment of the *Peridinium* patch is relatively fast. Taking into account the data collected during the morning – noon hours when the *Peridinium* population is concentrated into a thin layer 1-2 m below the water surface (see below) it is possible to ignore the vertical migration (that could be observed during the dark hours) and estimate the horizontal velocity of the patch. Based on T4 and T5 data maps, the horizontal velocity of the distinct patch identified in the north-west corner of the sampling grid at T4 was estimated to be 3 cm s^{-1}. The patch travelled a distance of ca 700 m during the 6 hrs interval until it almost disappeared at T5. The T0 data presented in Figure 5 provide another possibility to estimate the horizontal velocity of the patch. Although only part of the sampling grid is represented in T0, a dense patch was identified in the middle of the grid. Eight hours later, as T1 campaign was performed, the patch has practically moved away from the grid, representing horizontal velocity in the range of 5 to 7 cm s^{-1} depending on the direction of the patch migration.

Assuming that the horizontal velocity and the movment direction of the patch are directly affected by wind-driven currents, one may expect much stronger currents between T0 and T1 than between T4 and T5. Direct measurments of the wind vectors and velocities at several stations around the lake were applied in the ROMS model to predict the induced currents (see below A. Rimer and E. Shilo). The model predicted average current velocities of 5 cm s^{-1}, a value at the range of those calculated based on the chlorophyll data (Figure 5).

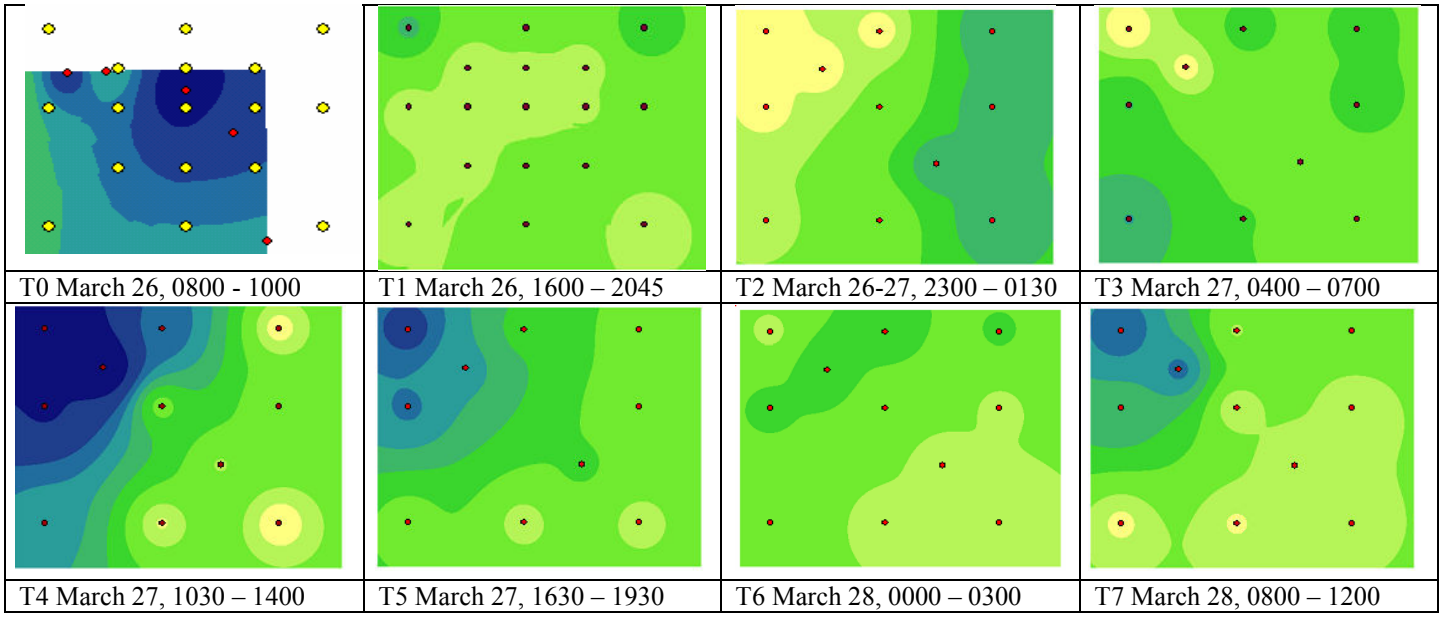

Color scale for chlorophyll concentration (mg m^{-3})

Figure 5: Spatial distribution of chlorophyll concentration at 1 m depth shown for 8 consequtive data acquisition campigns. Chlorophyll concentration ranged between 25 and 700 mg m^{-3}. Note that the T0 map is based on a preliminary data acquisition campaign. The sampling grid location and stations were determined based on that map.

The temporal variations in the horizontal distribution of chlorophyll (the signal of the *Peridinium* population) in a 1 m depth water layer (Figure 5) represent only two dimensions of the patchy phenomenon. The vertical aspect is better depicted by depth integration of the chlorophyll (fluorescence) signal to present maps of areal chlorophyll concentrations (Figure 6). The visual resemblance of chlorophyll maps presented in Figure 5 and 6 (1m layer concentration vs depth-integrated concentration) suggests 1) that the spatial variability is dominated by rapid horizontal movements of *Peridinium* patches and 2) that the fluorescence signal measured at 1 m depth predicts quite well the chlorophyll areal concentration.

The chlorophyll data acquired by the Fluoroprobe were further analyzed to present the vertical distribution of this parameter across a diagonal path (Figure 7) from station 1 to station 5 via three other sampling points (10, 17 and 14). The data presented in Figure 7 clearly indicates that during the day time the *Peridinium* population preferentially occupied the upper 3m layer (T4 and T7), while during the night time the population is dispersed across the upper 5-6 m (T2 and T6). Other sampling campaigns represent a variety of transition situations. In T1 only the edge of a *Peridinium* patch was recorded reaching a depth of 3 m to the most and chlorophyll concentration of 180 mg/m^3 at the most. T3 represents a relatively diluted population of *Peridinium* with chlorophyll concentration of 120 mg/m^3. In T5, the chlorophyll concentration along the diagonal cross section was rather low representing areas which are relatively free of *Peridinium* population with one exception at station 1 where high chlorophyll concentration was recorded at the top 3 – 4 m layer.

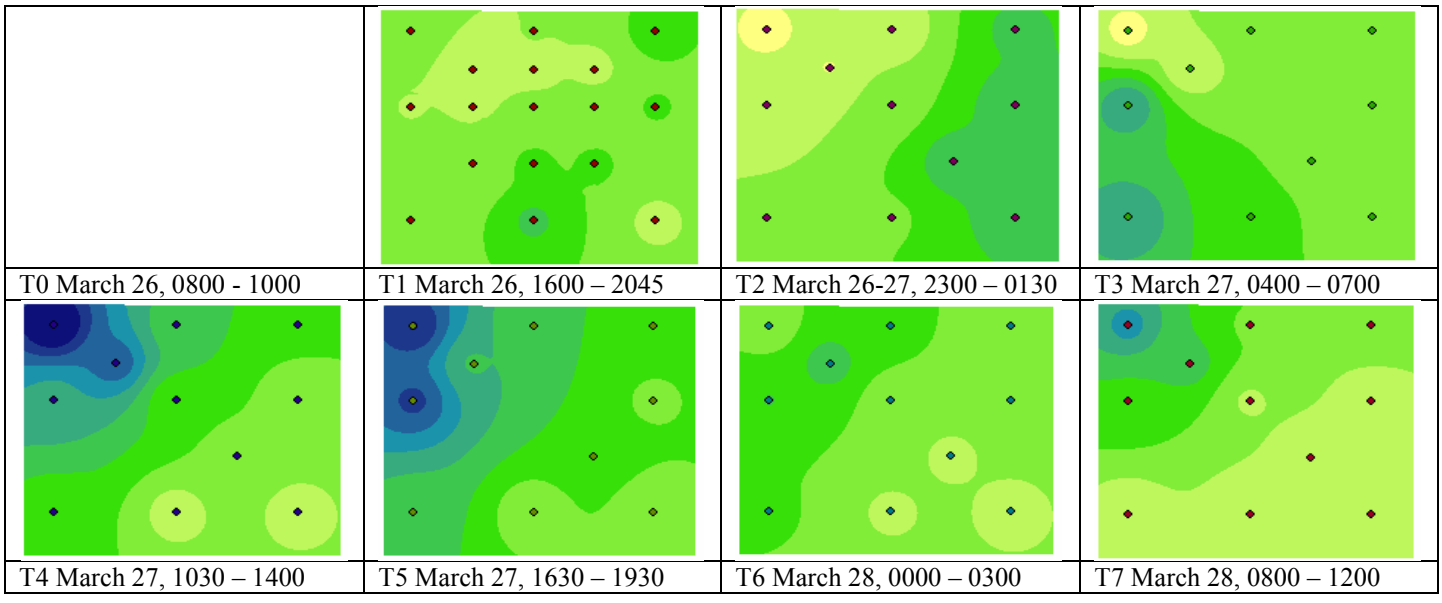

Figure 6: Spatial Distribution of depth-integrated concentration of chlorophyll in Lake Kinneret shown for 7 consequtive data acquisition campigns. Chlorophyll areal concentrations ranged between 200 and 2000 mg m^{-2}.

Color scale for chlorophyll concentration (mg m^{-2})

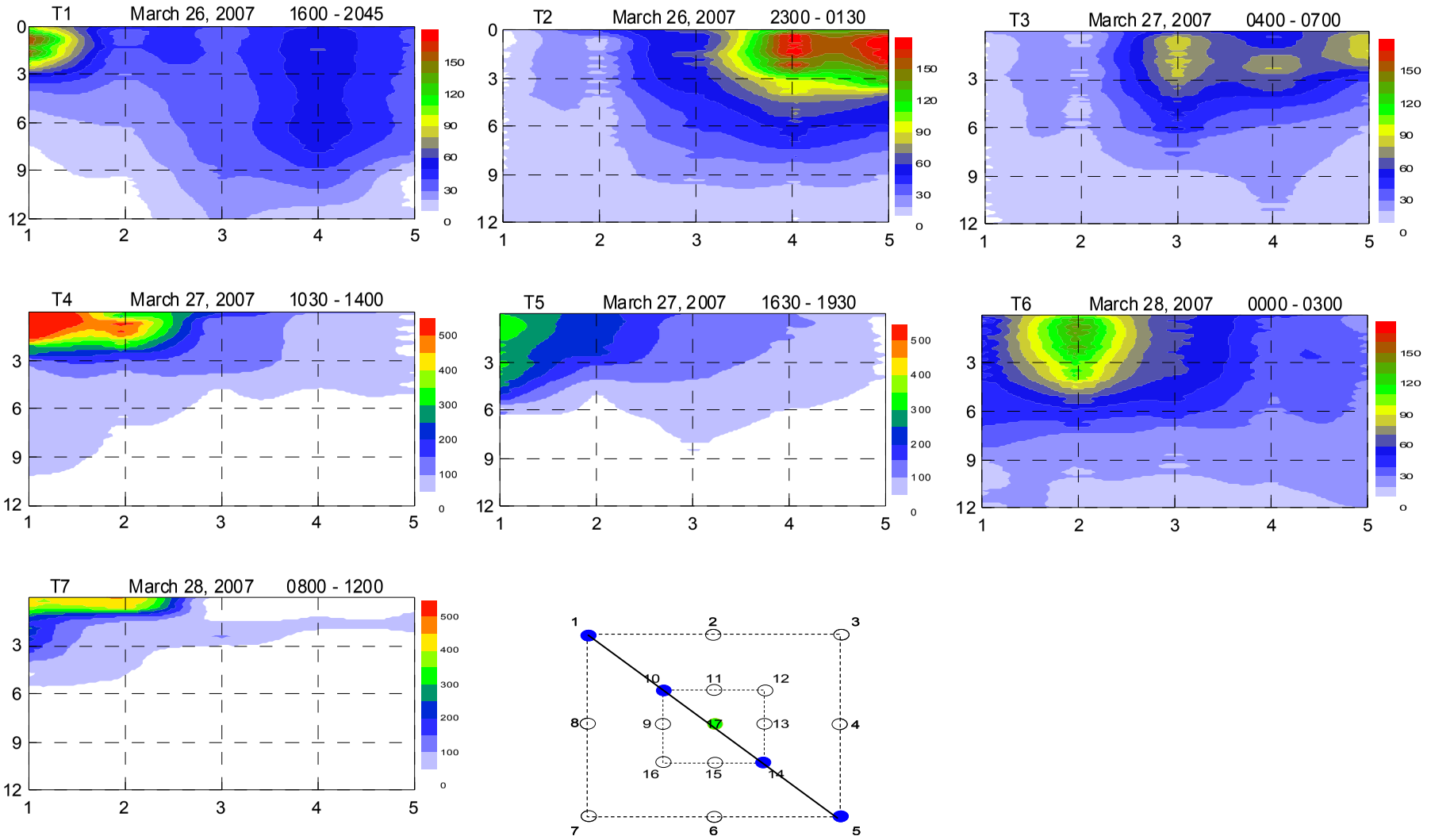

Figure 7: Vertical distribution of chlorophyll concentration (mg m^{-3}) (based on Fluoroprobe data) acquired at 5 sampling stations located on the diagonal line of the sampling grid. Data for each sampling campaign is shown in a quasi 3D format where y axis is depth, x axis the sampling stations (1=stn1, 2 =stn10, 3=stn17, 4=stn14, 5=stn5, as shown in the sampling grid). Each map represents a single sampling campaign from T1 to T7.

The vertical distribution (depth profiles) of *Peridinium* cells assumed multitude of shapes, ranging from a pretty uniform distribution throughout the entire uppermost 15 m of the water column, up to a massive concentrate at a limited depth interval, mostly close to the water surface or 1-2 m below the water surface (Figure 8). Typically, when a peak was seen at the surface, or just below the surface, Chl declined abruptly to low values (approximately 15% of the highest concentration) at a depth of about 5 m, and subsequently continued to decline mildly (Figure 9). The decline occurred at a deeper point, and less prominently in other cases, but it seems that Chl concentration at the base of the investigated water column (~ 15 m) was not related to the density found in the euphotic zone, and mostly did not surpass 15 mg m^{-3}.

Maximum Chl concentration ranged from 14 to 799 mg m^{-3} (Table 2). Interestingly the degree of variation in vertical Chl distribution was positively correlated with the log transformed maximum Chl concentration (Figure 10). This trend indicates temporal concentration pattern of the population that occurs at a relatively narrow water layer during the day time. Thus the finding reflects the situation that Chl profiles with a prominent peak (e.g., T2 at Stn3 in Figure 8) were mostly formed on occasions when Chl, concentrations were >100 mg m^{-3}. The temporal and spatial variability of Chl maximum was high, showing coefficients of variation between 38 (Stn 17) and 110% (Stn 1), and between 74 (T1) and 311% (T4), respectively.

The maximum concentration of Chl was pretty closely correlated with the concentration of Chl seen at the uppermost 0-1 m (Figure 11). Thus we conclude that the measurement of chlorophyll concentration at 1 m depth reflected the maximal chlorophyll concentration in the entire water column although the depth of the chlorophyll layer substantially varied between day and night.

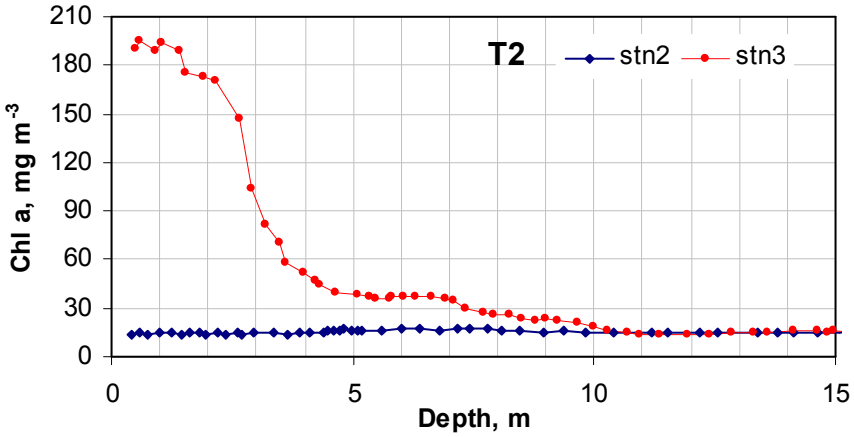

Figure 8: Vertical distribution of Chl *a* at two stations of T2. FP profiling started on (26 March 2007) 23:25 at Stn 2 and 12 min later at Stn 3, ca 1500 m away from station 2. The profiles present two locations, one inside (Stn3) and the other outside (Stn2) the *Peridinium* patch.

Table 2: Maximum Chl *a* concentration (mg m^{-3}) in each of the sampling campaigns and stations.

Station	T1	T2	T3	T4	T5	T6	T7
stn1	162	14	36	799	348	45	417
stn2	81	17	113	438	139	137	68
stn3	138	195	105	220	73	120	85
stn4	92	186	112	116	59	45	86
stn5	39	190	94	51	42	29	61
stn6	79	54	105	49	38	38	46
stn7	49	41	207	352	81	74	39
stn8	46	18	156	632	262	110	303
stn10	33	15	18	572	217	149	515
stn14	63	188	86	80	115	36	71
stn17	38	54	91	109	119	63	114

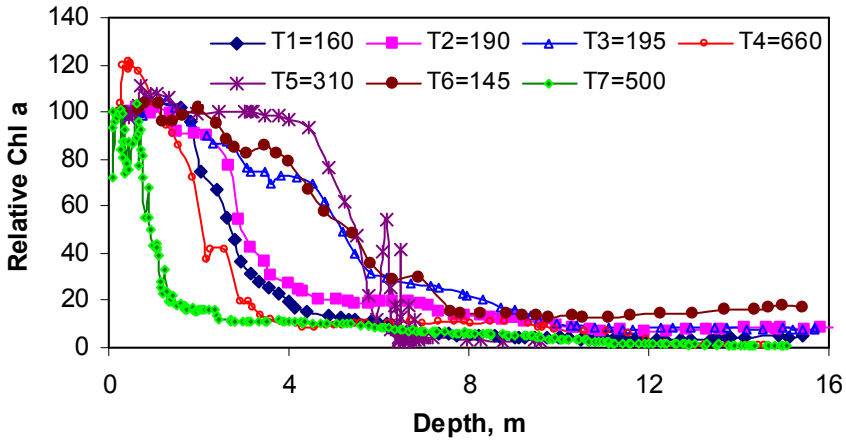

Figure 9: The vertical distribution of Chl *a* at stations with the highest concentration in each one of the 7 sampling campaigns conducted in Lake Kinneret on 26-27 March 2007. Values are relative concentrations of Chl *a*, when the uppermost measurement is 100% for each profile (i.e. 0-0.5 m depth sample). The legend indicates the campaign number (T1….T7) and Chl *a* concentration of the uppermost measurement, in mg m^{-3}.

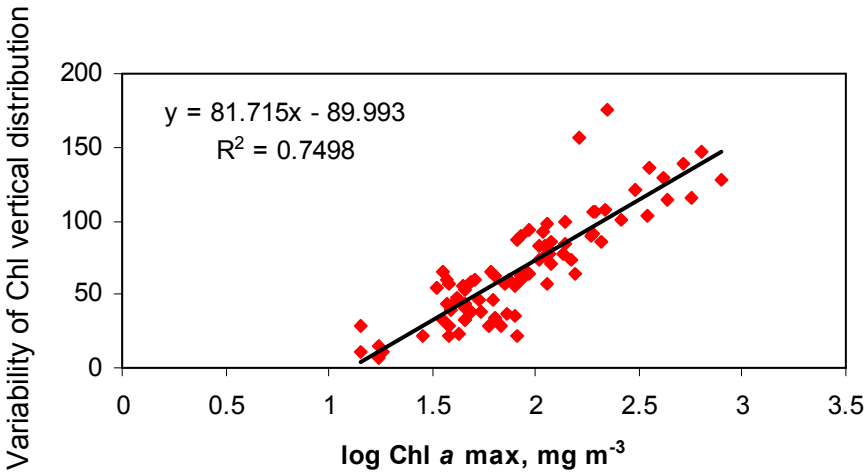

Figure 10: Relationship between maximum Chl *a* concentration (log transformed) and the variability of vertical distribution of Chl (expressed as coefficient of variation).

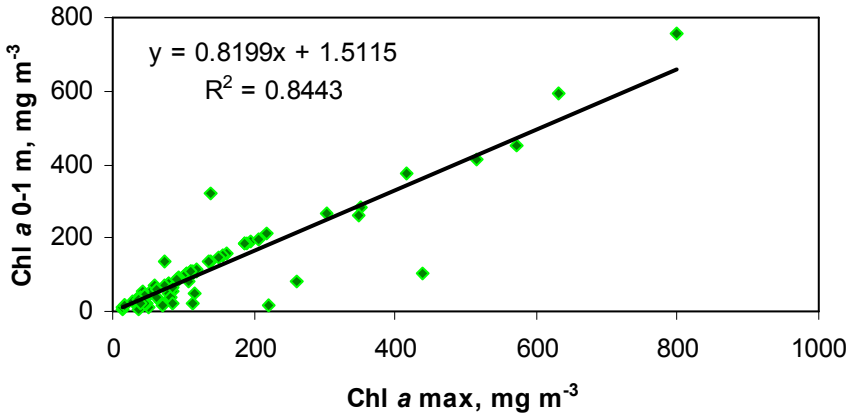

Figure 11: Relationship between Chl a maximum concentration and the concentration of surface Chl (0-1 m) at 11 stations and 7 sampling campaigns in Lake Kinneret. Chl *a* concentration was determined by FloroProbe *in situ* measurement from 26 to 28 March 2007.

2. Under-water towed undulating monitoring system (U-TUMS) revealed the dynamic properties of Peridinium patches (Assaf Sukenik)

Four independent surveys were performed by the U-TUMS. The first and the last surveys were carried out during early afternoon while the two others were performed around midnight (see Table 1). Due to technical problems the U-TUMS was not operated at near water surface thus the upper most data was collected at 1 m below surface. With this constraint the chlorophyll maximum during the day light is partly missed as presented in the chlorophyll profiles in Figure 12.

The first (T1) U-TUMS operation was carried out on a west east transect and back on the same latitude line, 32.862 E, which represents the northern part of the sampling grid. The fluorescence maps shown in Figure 12 indicate substantial differences between the W to E transect (Figure 12A) and the backward E to W transect (Figure 12B). In the first transect, high fluorescence signal (red color) was identified in the upper 1 m layer along its eastern part. In the backward transect the fluorescence signal was decreased but substantially dispersed to a thicker layer and could be found along the entire transect (Figure 12B). Due to the 2 dimensional nature of the geographic data, it is rather impossible to assess the dynamic of the fluorescence signal dispersion that reflects the migration and distribution of the *Peridinium* population. However it is clear that the observed changes occurred within the range of one hour, the time required to run a single transect.

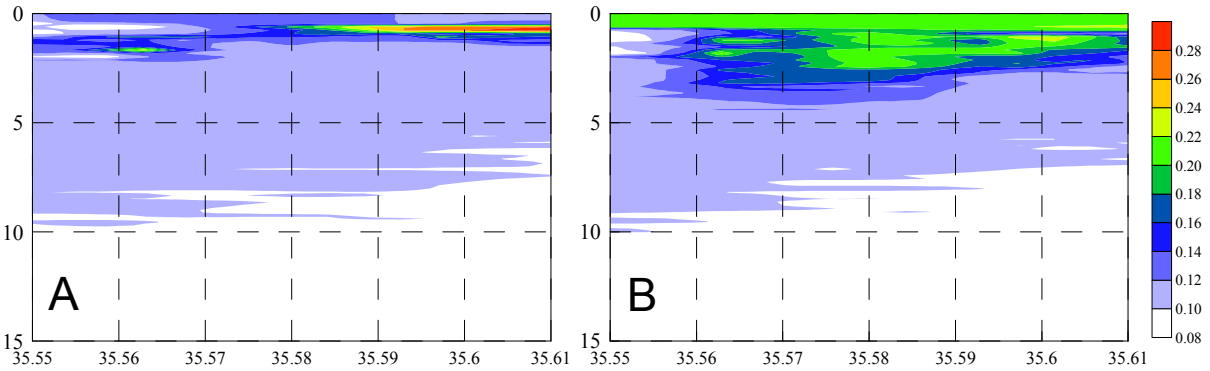

Figure 12: Vertical distribution of chlorophyll fluorescence signals acquired by the Underwater Towed Undulating Monitoring System operated at T1 on a west east transect (A) and back (B) on the same latitude line, 32.862 E, which represents the northern part of the sampling grid. Data are shown in an integrated quasi 3D format where y axis is depth x axis is the longitude and the chlorophyll fluorescence signal, in mg m^{-3}, is depicted by colors as presented in the color scale.

Another example of such a rapid dynamic of the patch dispersion and translocation is provided in Figure 13 depicting the fluorescence signal acquired along W-E transect and back on latitude line, 32.842 E which was about 800 m southern to the line of stations 5 to 7 of the sampling grid. Although the presented U-TUMS data cannot be directly associated with the chlorophyll measurements collected at the sampling grid, it demonstrates the rapid dynamics of the patch. The data collected around midnight (T5) show that the patch identified along longitude lines of 35.545 and 35.58 E penetrated to 2 m in the water column (Figure 13A). About 1 hour later the patch dimensions were changed, stronger fluorescence signals were recorded at the center of the patch and it was located at a deeper layer (Figure 13B).

These changes are interpreted as a result of two different processes which are mutually exclusive, the horizontal movement of the population facilitated by wind driven currents, and vertical movement, presumably associated with the motility of *Peridinium*. The reconstruction of 3 dimensional distribution of the *Peridinium* population that may help understand the changes in the patch structure is rather complicated. However with several simple assumptions, the velocity of the downward vertical vector is estimated as 0. 5 mm s^{-1} (2 m divided by 1 hr).

Given that we know the dimensions of a *Peridinium* cell one can calculate the free falling velocity of the cell in the water column based on Stokes equation:

$$V_s = \frac{g}{18} \times d^2 \times (\rho_p - \rho_l) \times \eta^{-1}$$

Where V_s – Settling velocity ($m \cdot s^{-1}$), g – gravitational acceleration force (9.81 $m \cdot s^{-2}$), d- cell diameter ($60 \cdot 10^{-6}$ m), ρ_p – specific density of the paricle (1090 $Kg \cdot m^{-3}$), ρ_l - specific density of the liquid (997 $Kg \cdot m^{-3}$), η - dynamic viscosity of the liquid (0.00095 $Kg \cdot m^{-1} \cdot s^{-1}$).

Based on the specified values of these parameters we estimated the settling velocity of *Peridinium* to be 0.2 $mm \cdot s^{-1}$. This value is at the same order of magnitude as the value estimated from what we presume as the patch vertical migration (Figure 13).

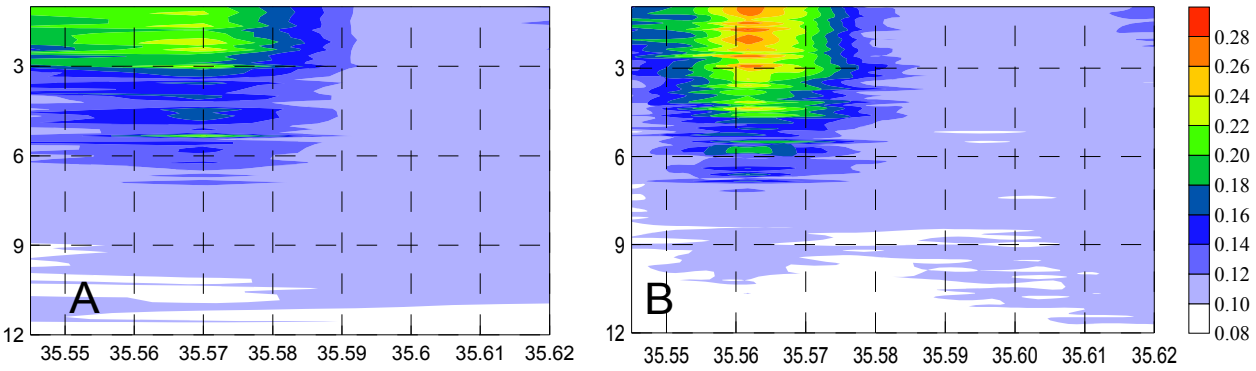

Figure 13: Vertical distribution of chlorophyll fluorescence signals acquired by the Underwater Towed Undulating Monitoring System operated at T3 (near midnight) on a west east transect (A) and back (B) on the same latitude line, 32.842 E which was about 800 m southern to the line of stations 5 to 7 of the sampling grid. 32.862 E, which represents the northern part of the sampling grid. Data are shown in an integrated quasi 3D format where y axis is depth (m) x axis is the longitude and the chlorophyll fluorescence signal (relative units) is depicted by colors as presented in the color scale.

3. *Morphological characteristics of the Peridinium population (Tamar Zohary, Alla Alster, Tatiana Fishbein)*

Methods

Discrete-depth water samples for *Peridinium* cell counts and linear measurements were collected at all 'biology stations' and sampling depths, and preserved with Luogl's solution. Of those, representative samples were chosen for counting and cell diameter measurements. Those samples were taken from within, below or outside the patch as indicated by the Fluoroprobe Chl concentration and at different times of the day and night (Table 3). Measurements were made on the first ~100 *Peridinium* cells encountered in each sample with PlanktoMetrix software package. In addition to the Lugol-preserved samples, live and Formalin-preserved subsamples of selected samples were brought to the lab for microscopic examination. Based on the literature (Pollingher & Serruya 1976, Pollingher 1988) we expected cell division to take place in the upper part of the water column at night, and examined our samples microscopically immediately after sampling, especially those collected at night.

Results

Peridinium biomass, based on cell counts on discrete-depth samples multiplied by cell volume as computed from the linear measurements, correlated extremely well (R^2=0.989) with the fluorescence signal for dinoflagellates measured by the Fluoroprobe (Table 3, Figure 14). This suggested that the Fluoroprobe data provide an accurate estimator of *Peridinium* abundance in the water column.

We recorded a relatively large size variability (Figures 15, 16) in a total of > 1600 *Peridinium* cells measured, cell diameter ranged from 35.1 to 65.3 μm, with 49.6 μm as the mean and 49.1 μm as the median. The intermediate sizes, between 45 – 55 μm contributed about 80% of the population (Figure 17), but there was still a substantial population of particularly large (hence 'giant') and particularly small cells. Our microscope observations indicated that the 'giant' cells are the ones about to undergo cell division, while daughter cells that just emerge out of their

mother thecae are the smallest cells in the population (Figure 16). Thus, the large size variability observed is indicative of an actively growing population.

Table 3: Samples chosen for *Peridinium* cell size analysis, number of cells measured, the FP-recorded Chl concentration and the *Peridinium* wet-weight biomass, based on the cell counts and linear measurements [there are 6 more samples to add to this list]

Date	hour	Sampling Time	Sta	Depth	# cells measured	FP Chl, ug/L	*Peridinium* mg/L
27-Mar	00:05	T2	5	1	56	182	70.2
27-Mar	00:20	T2	5	15	92	11	2.5
27-Mar	17:00	T5	1	1	101	337	161.0
27-Mar	19:35	T5	17	1	122	116	55.9
27-Mar	19:45	T5	17	7	122	68.3	20.0
27-Mar	19:55	T5	17	15	85	10.7	3.5
28-Mar	00:15	T6	10	1	54	148	62.0
28-Mar	03:30	T6	14	1	150	33	8.2
28-Mar	02:40	T6	17	1	101	56	12.9
28-Mar	02:50	T6	17	7	77	27.5	9.9
28-Mar	03:00	T6	17	15	52	13.5	3.7
28-Mar	08:30	T7	1	1	101	330	144.0

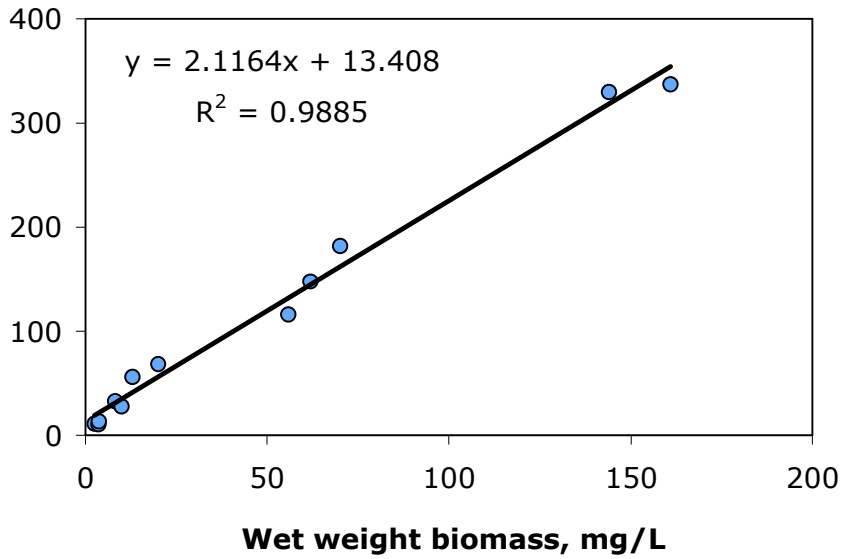

Figure 14: A strong linear relationship existed between the wet-weight biomass of *Peridinium* and the Fluoroprobe readings in the water column.

Figure 15: Large variability in *Peridinium* cell size

Our night observations of fresh material confirmed previous observations by Serruya and Pollingher (1976) that *Peridinium* cell division takes place mostly between midnight and 4 am. We observed cells at various stages of mitotic cell division, from the duplication of the chromosomes and the separation of the nucleus into two nucleii at two sides of the cell (seen as an S-shaped nucleus) to the final emergence of 2 daughter cells leaving behind an empty theca (Figure 16).

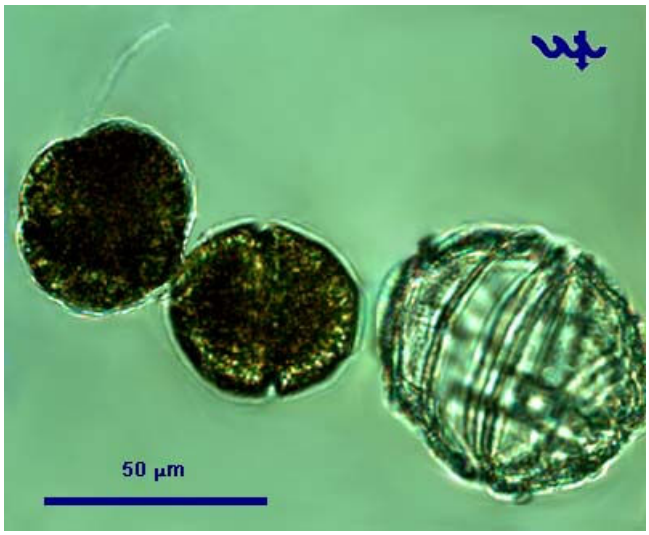

Figure 16: Two small daughter cells that just emerged out of the mother thecae.

Based on the size distribution presented in Figure 17, we defined cells < 45 µm as 'small' (S) and cells > 55 µm as 'giant' (G). On average, S cells constituted 11.4 % of the entire population, G cells constituted 10.25%. We used their sum G+S, expressed as % of the total number of cells in the population as an indicator of the proportion of the population that is actively dividing.

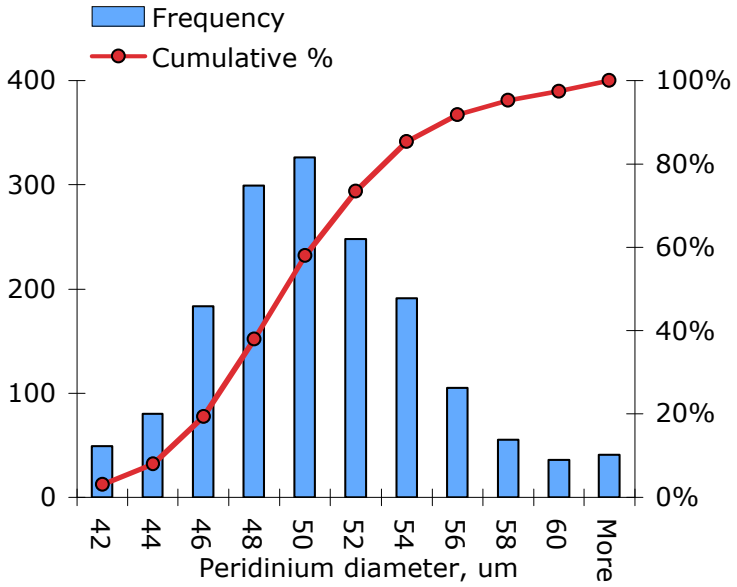

Figure 17: Frequency histogram of cell diameters of *Peridinium* sampled during 27-28 March 2007, sample info is given in Table 1. X-axis shows the size in um of the largest diameter falling in the size class, so 42 refers to cells < 42 µm, 44 refers to cells ≥42 and <44 µm etc.

We found strong correlations between various environmental factors and %G+S (Figures 18, 19). Of particular interest was the strong negative correlation between conductivity and % G+S (R^2=0.588), suggesting that `` River water (low conductivity) stimulate growth of *Peridinium*. Other factors correlated with %G+S or stimulating growth were shallow depth (R^2=0.46), high population density as indicated by Chl concentration (R^2=0.73), warmer temperatures (positive correlation, R^2=0.75), higher DOC (R^2=0.74), higher SRP (R^2=0.38) and lower alkalinity (R^2=0.52).

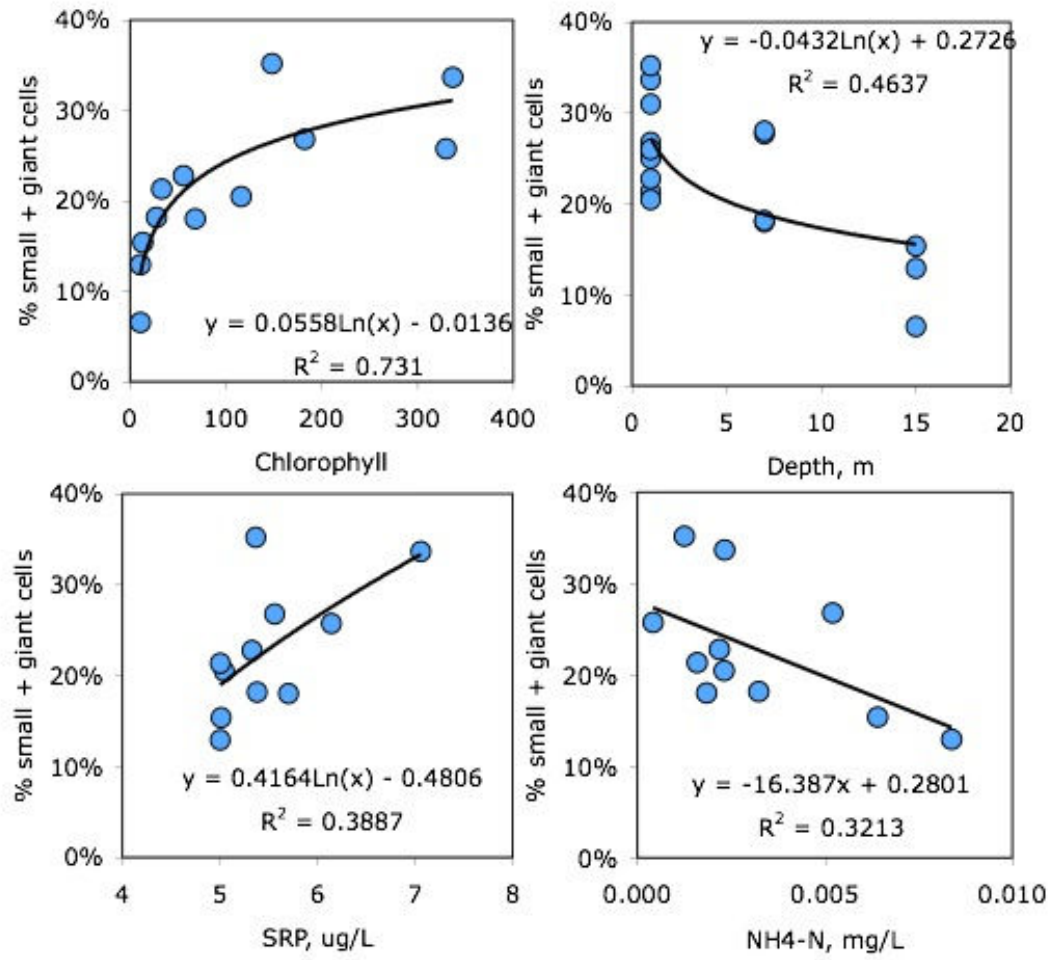

Figure 18: The relationship between various environmental parameters and the % of very small and giant cells in the population, indicative of cell division.

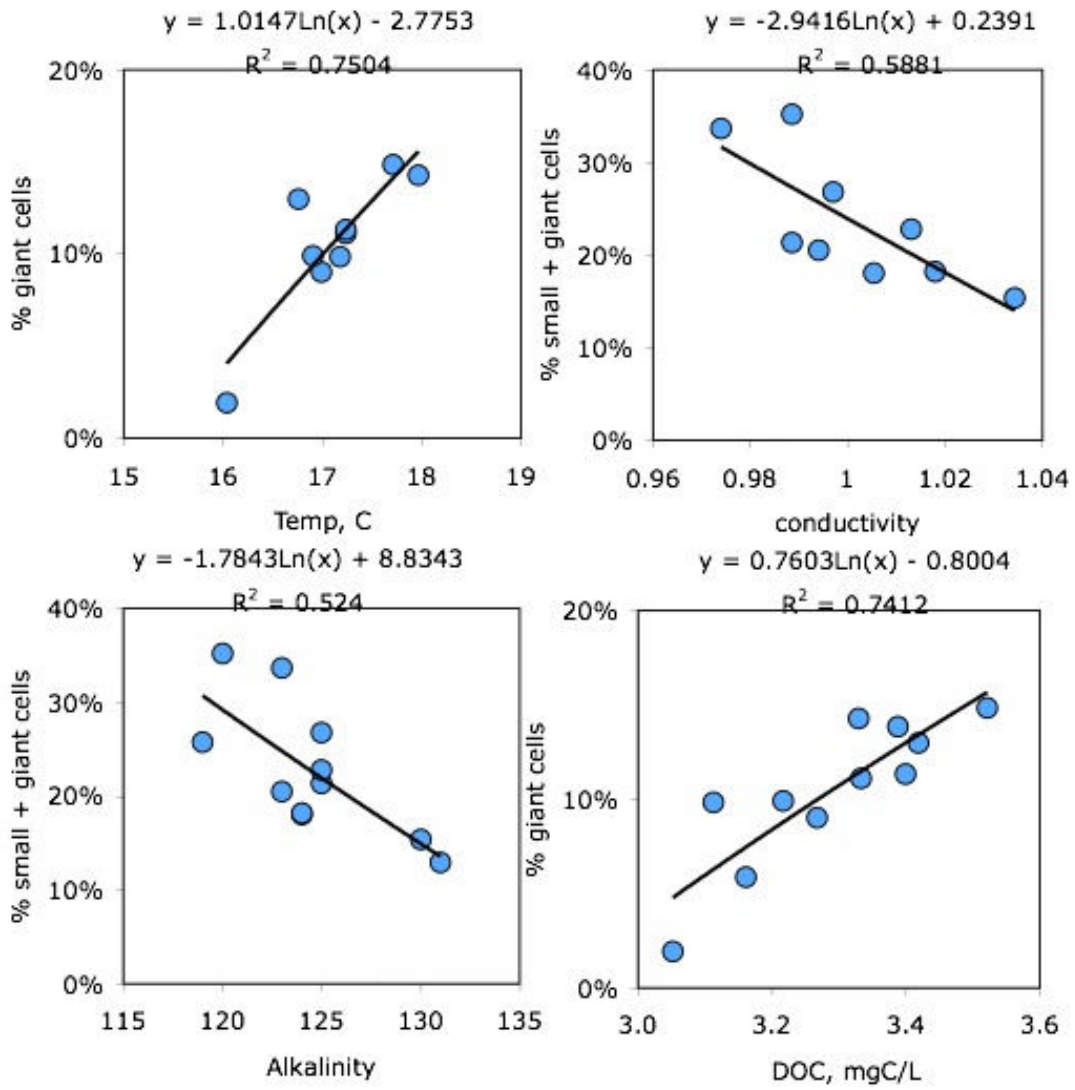

Figure 19: Same as Figure 18 for additional environmental parameters.

4. Zooplankton (Gideon Gal and Sara Chava)

Methods

Zooplankton samples were collected at discrete depths at a number of stations (see Table 4 for complete listing). Samples were collected using a 5-L bottle sampler. Samples were fixed on board the boat with buffered Formaldehyde 36%. Once at the laboratory, and at least 24 hrs latter, samples were concentrated and transferred to vials and preserved with Ethanol 70% + Glycerin 1%. Only a subsample of the complete array of samples were analyzed and counted and included samples from transects 4 and 5 at depths of 1 and 7 m and at stations 1, 5, 10, and 14 (Table 4). Of the concentrated samples, between 0.5-15 ml were removed and counted. This represented between 0.7-60% (24% on average) of the total sample. The samples were counted, under a microscope, and aggregated according to general taxonomic groupings of life stage groups as follows: adult copepods, copepodites (C1-CIV), nauplii, cladoceran, and rotifers.

The count results were binned according to functional groups: predators, herbivores, and microzooplankton. The first group included adult cyclopids, the second group included the

cladocerans and copepodites and the microzooplankton included rotifer species and nauplii. All analyses were performed based on the functional groups.

Table 4: List of stations and depths at which samples were collected. The sampling was identical over the course of all transects. Samples were counted only for transects 4 and 5.

Station	Depths Sampled (m)	Counted?
1	1	Y
	7	Y
	15	N
5	1	Y
	7	Y
	15	N
10	1	Y
	7	Y
14	1	Y
	7	Y
	15	N
17	1	N
	7	N
	15	N

Results

Samples analyzed indicated a heterogeneous distribution of zooplankton over the sampling area and over time. The densities of microzooplankton, for example, varied between 8 individuals L^{-1} up to over 2,000 individuals L^{-1}, over a 250-fold increase. Changes in the herbivore and predator densities were not as extreme and ranged between 7-166 herbivores L^{-1} and >1 – 157 predators L^{-1}, respectively. Most notable, however, was the variation between stations (Fig. 20). The highest densities of microzooplankton were found at station 1 at a depth of 1 m during transect 4 (2079 individuals L^{-1}) and at a depth of 7 m during transect 5 (1636 individuals L^{-1}). Densities at other times/depths at station 1 and at all other stations were considerably lower with values below 784 individuals L^{-1}. In fact, densities at stations 5, 10 and 14 during both transects and at both depths did not exceed 500 individuals L^{-1} with only two exceptions (Fig. 20).

The highest overall densities of both the predators and herbivores were found, with few exceptions; during transect 4 at a depth of 7 m (Fig. 21). On the other hand, their lowest density was found during the same transect at a depth of 1 m with only two exceptions. While the herbivores were most abundant at station 1, especially during transect 4, there was no clear pattern in the predator distribution.

We examined the impact of time of day on the vertical distribution of the zooplankton. There was a clear difference between the morning transect, t4 (1030 – 1400) and the afternoon transect, t5 (1630 – 1930). During the morning transect, with only few exceptions of mainly station 1, zooplankton densities were notably higher at a depth of 7 m than at 1 m (Fig. 22). This pattern did not remain, however, during the afternoon transect. During the latter transect there was no clear pattern in the depth distribution with similar densities at both depths.

The large peak in microzooplankton and herbivores at a depth of 1 m at station 1 during transect 4 coincides with the patch of *Peridinium* occurring at the same location and time. The differences in densities between that depth and station at that point in time to other sampling

locations and times are striking. Microzooplankton density at that station and time of sampling was approximately 27% higher than the closest point but 4.3 times higher than the average of all other points. In the case of the herbivores, the peak density at 1 m at station1 during transect 4 was 2.5 times higher than the mean value of all other points.

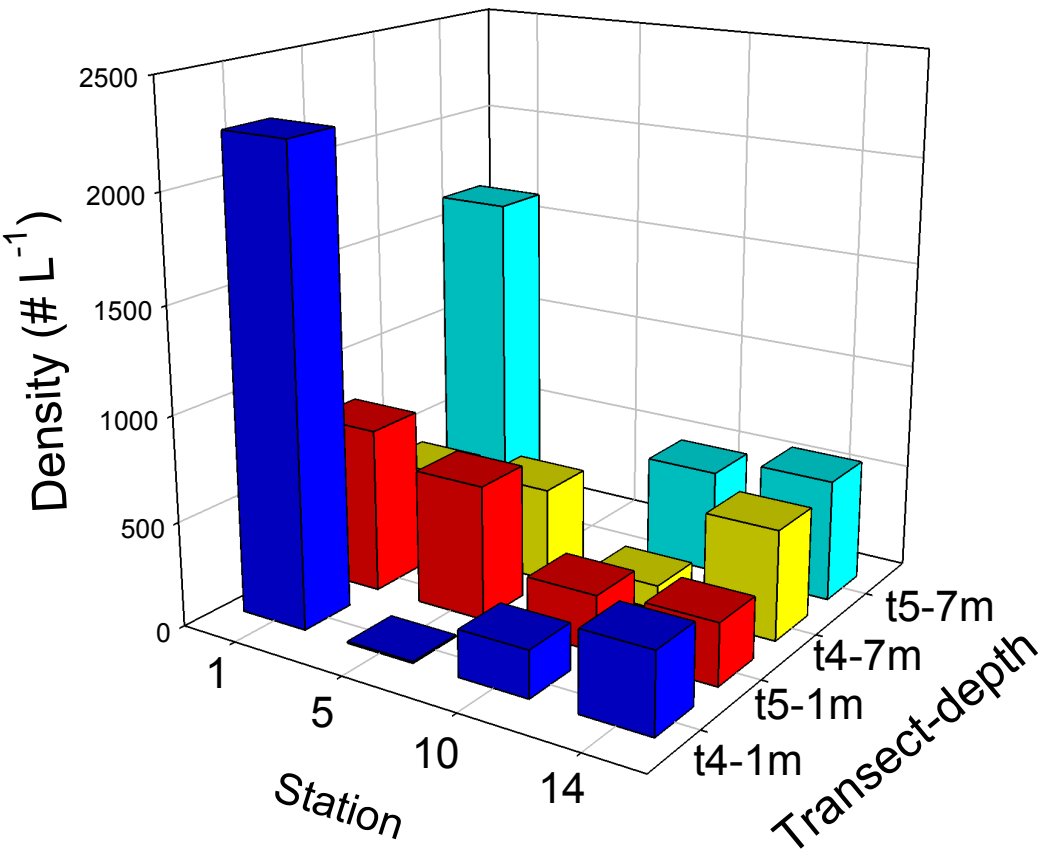

Figure 20: Microzooplankton densities during transects t4 and t5 at stations 1, 5, 10 and 14 at depths of 1 and 7m.

Thus, that point in time and space represented a patch of increased microzooplankton and herbivorous zooplankton. This was not the case, however, for the predatory zooplankton (adult cyclopoids). It is difficult to determine from the data whether the *Peridinium* and zooplankton were in the patch for the same reason, e.g. linked to the Jordan River inflow or whether one of them was there because of the other. Undoubtedly, the *Peridinium* benefits from the high densities of zooplankton in the patch. While they are not exposed to predation pressure by zooplankton due to their large size, they can enjoy the nutrients excreted by the zooplankton. If we roughly estimate the amount of N and P released by zooplankton to the water, within the patch, using the estimated densities converted to wet weight (based on the KLL database conversion factors) and carbon (assuming a C:WW=0.08) and using published excretion rates for Lake Kinneret (Hambright et al 2007) we find estimated average excretion rates of 435.1 µgN L^{-1} d^{-1} and 58.1 µgP L^{-1} d^{-1}. These values are high especially if we consider the average concentration of SRP at the same station and time was 11.9 µg P L^{-1}. In the case of nitrogen, ammonium values were low (<10 µgN L^{-1}) and nitrate was estimated at 1.78 mgN L^{-1} d^{-1}. If we further assume a phosphorus uptake rate by *Peridinium* ranging between 0.0006 and

0.009 mgP mg C^{-1} d^{-1} (Zohary and Makler 2004) than the estimated contribution by zooplankton to the phosphorus uptaken by *Peridinium* in the patch ranges between 149 and 10% of their daily needs. The large range is a result of the > 1 order of magnitude range in reported P uptake by *Peridinium* (Zohary and Makler 2004). The calculations are only gross estimates as a number of assumptions were made however they do indicate a significant impact the zooplankton may have on the *Peridinium* population. While the relationship is not in the form of top-down control since there is no predator-prey interaction between the zooplankton and *Peridinium* there is a form of bottom-up control due to supply of nutrients by the zooplankton.

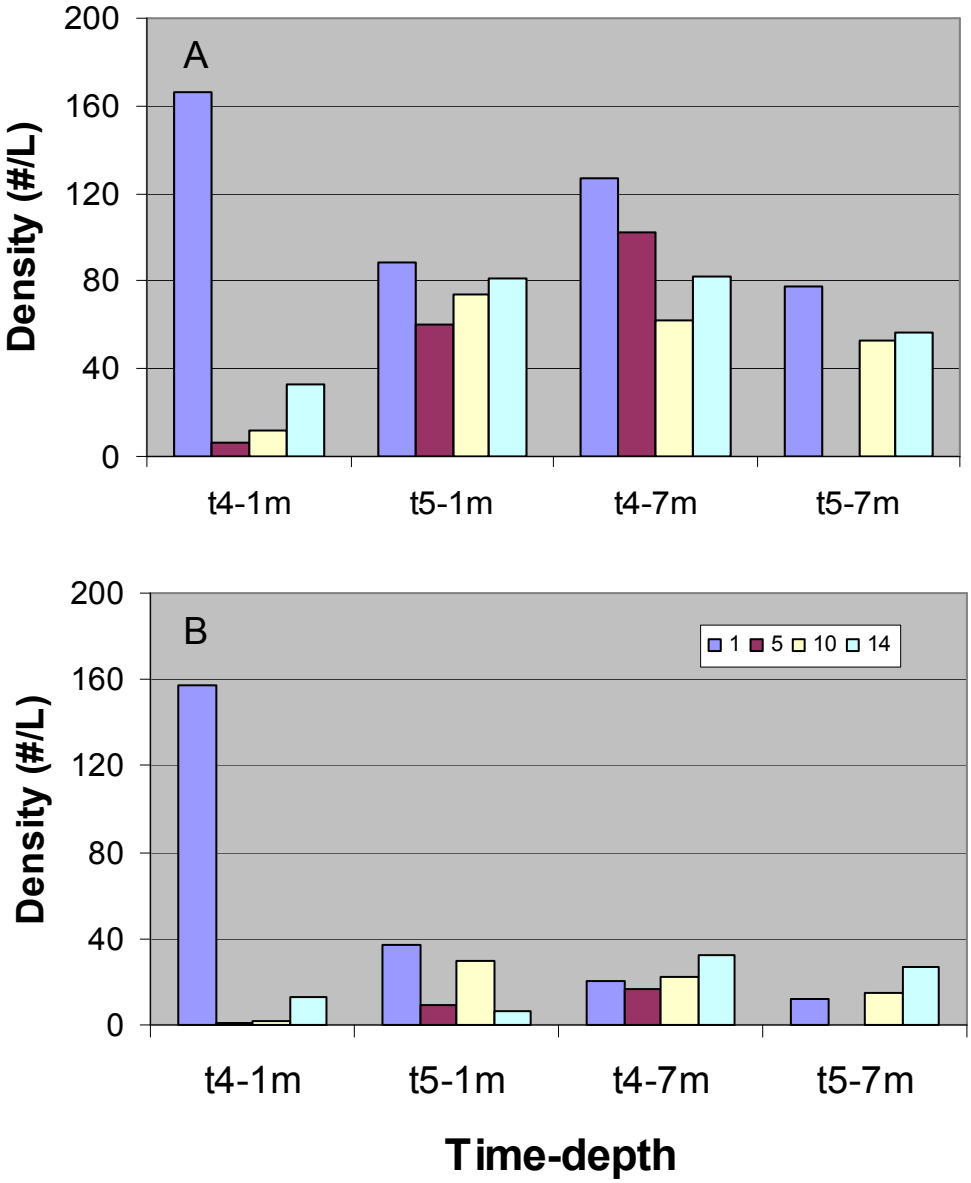

Figure 21: Herbivorous (A) and predatory (B) zooplankton densities during transects t4 and t5 at depths of 1 and 7 m at four stations: 1, 5, 10, and 14.

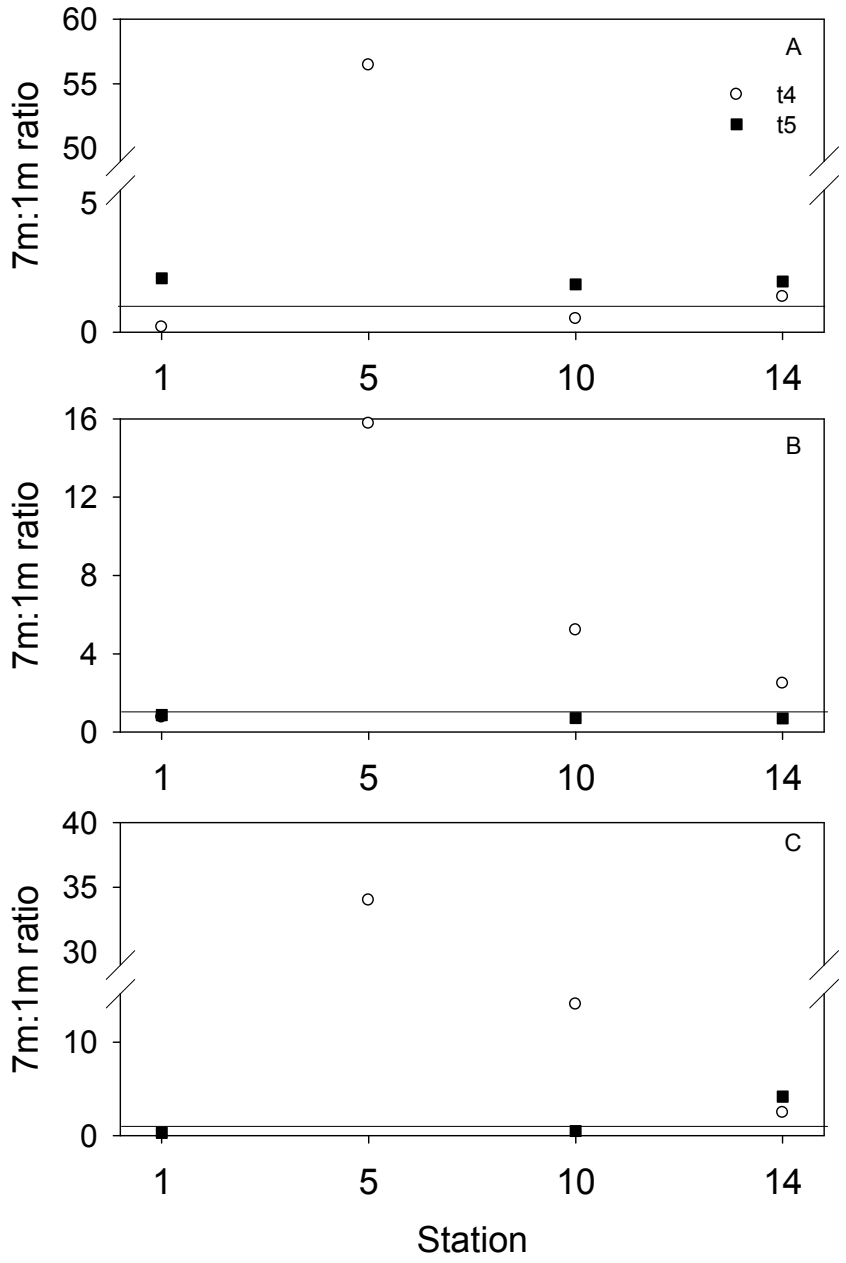

Figure 22: The ratio between the density of zooplankton at 7 and 1m during the T4 (open circles) and T5 (filled squares) sampling campaigns at four sampling stations: St 1, St 5, St 10, and St 14. (A) microzooplantkon (B) herbivorous zooplankton and (C) predatory zooplankton. The horizontal line represents a value of unity. Values greater than unity indicate higher densities at a depth of 7 m. Values for stations at which densities were 0 were removed from the calculations.

5. Cellular composition (Werner Eckert)

The cellular composition of *Peridinium* was characterized via the determination of particulate organic carbon (POC), nitrogen (PN) and phosphorus (PP) in water samples. For POC and PN analysis two 50- 100 ml subsamples were filtered through 13 mm pre-combusted GFF filters followed by drying at 70°C. In order to remove inorganic carbon from the particulate matter, filters were exposed to an acid atmosphere by placing them for 48 hours in a dessicator together

with a beaker containing 37% HCl under vacuum. After the acid treatment the filters were tranferred into silver capsules, sealed and anlyzed for carbon and nitrogen on a CHN elemental analyzer (PERKIN ELMER, PE 2400). Using standard analytical procedures (APHA, 2005) PP was calculated as the difference between total (TP) and total dissolved (TDP) phosphorus both measured spectro-photometrically in unfiltered and filtered subsamples respectively.

As in the case of Chl.a (6 – 670 µg l^{-1}) the analysis of parallel water samples revealed a large variabilty with concentrations ranging from 0.5 – 65 mg C l^{-1} in the case of POC, from 0.01 – 4 mg N l^{-1} for PN and from 0.5 – 517 µg P l^{-1} for PP.

In order to arrive at a representative value for the composition of *Peridinium* cells molar element concentrations were plotted against the weight of chlorophyll for those samples with chl a > 70 µg l^{-1} (Fig. 24). Based on the slope of the resulting regression lines it can be concluded that during the time period of the experiment the *Peridinium* population contained for each µg of Chl a approximately 12 nmol P, 410 nmol N and 6.3 µmol of C, corresponding to a C:N:P ratio of 522:34:1, within the range reported by Wynne et al. (1982) and somewhat higher than the ratio determined by Zohary et al. (1998) .

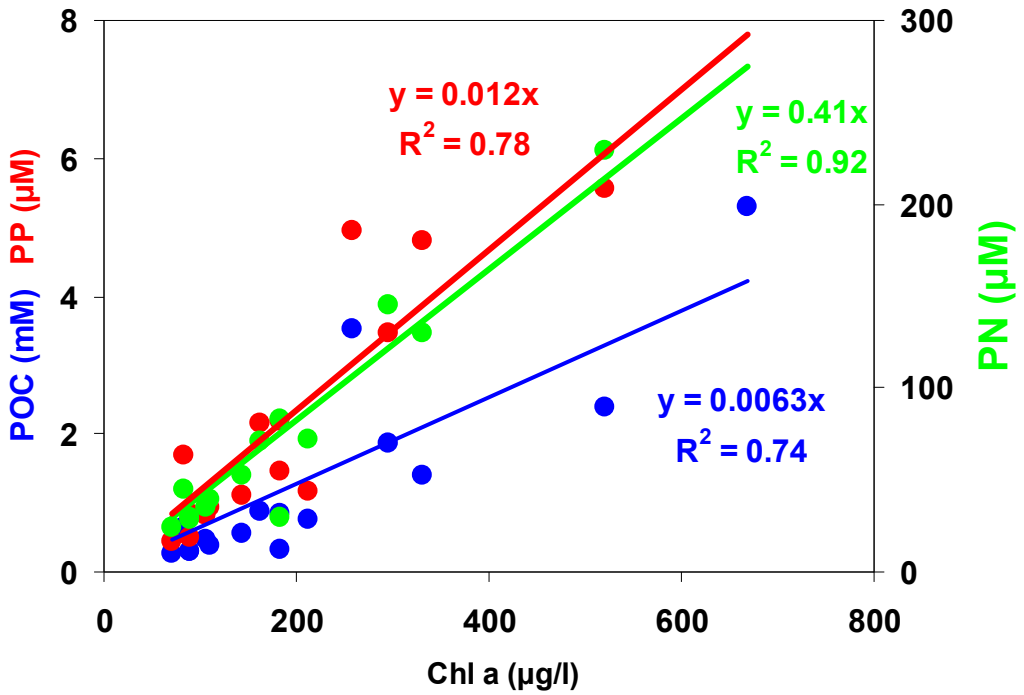

Figure 23: The ratio between chlorophyll concentration and elementary composition of the particulate material. Only samples with chl a > 70 µg l^{-1} are presnted in order to specifically analyze *Peridinium* cells.

6. Other biological parameters - Alkaline phosphatase activity, photosynthesis and community respiration (Ora Hadas, Arkadi Parparov, David Wynne, Yossef Yacobi).

Only two parameters of cellular activity were measured during the *Peridinium* operation of 2007, one, the activity of the hydrolytic enzyme alkaline phosphatase at all times and stations, and the second, community respiration at T1 and T4 (see below).

a. Alkaline phosphatase activity

Highest alkaline phosphatase activity was measured at Stn 1 on T4 reaching values of 606 nmoles MU l^{-1} h^{-1} with corresponding chlorophyll values of 669 µg chl l^{-1}. The total activity in nmoles MU l^{-1} h^{-1} at all times is presented in Figure 24A and the activity per µg chl in Figure. 24B.

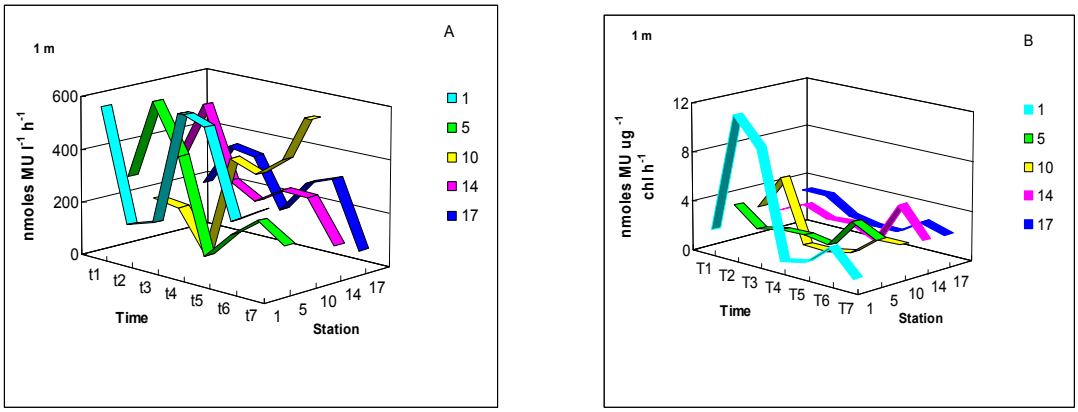

Figure 24: Alkaline phosphatase total (algal and bacterial) activity at 1m depth at various stations and times A – activity expressed in nmoles MU l^{-1}, B: activity expressed in nmoles MU µg Chl^{-1} h^{-1}.

The highest chlorophyll values i.e. the highest *Peridinium* biomass was associated with maximum total enzymatic activity, but per chl unit the activity was the lowest (0.67 nmoles MU μg^{-1} chl h^{-1} at 1m depth at Stn 1 at T4 as compared to 11.54 nmoles MU μg^{-1} chl h^{-1} at 1m depth at Stn at T2). At stations where the patch was prominent (usually during light hours) the activity at 1 m depth was higher as compared to Apase activity at 7 m depth.

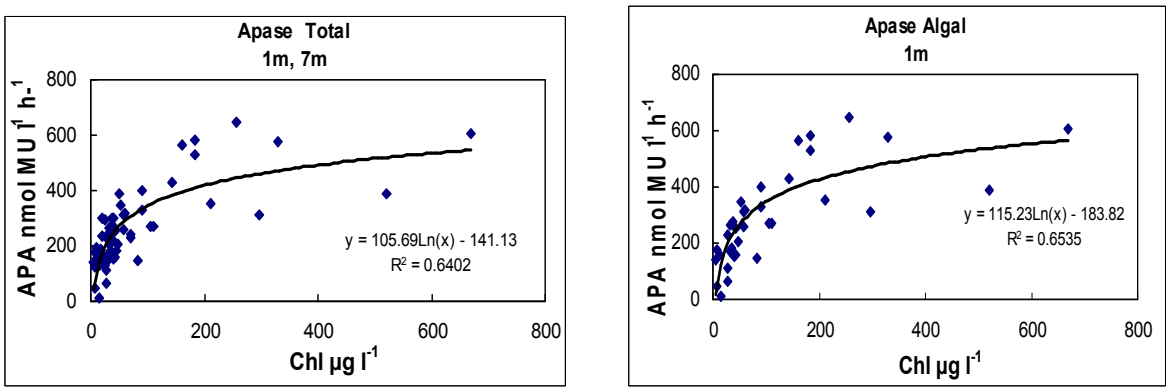

Figure 25: Correlation between chlorophyll and total Apase activity at 1m and 7 m at all stations (left hand panel), and algal activity at 1m (right hand panel).

Analyzing the relationships between Apase activity and chlorophyll (Figure 25) it is clear that at chlorophyll values above 300 µg Chl L^{-1}, characteristic of a patch, there is no increase in alkaline phosphatase activity with increase of biomass, explaining the low activity values monitored at chlorophyll maxima (i.e 1m depth at Stn1 at T4 Figure 24B). Omitting samples with chlorophyll values above 300 µg Chl L^{-1}, and studying the correlations, showed that increase in chlorophyll resulted in a linear increase in Apase activity (Figure 26).

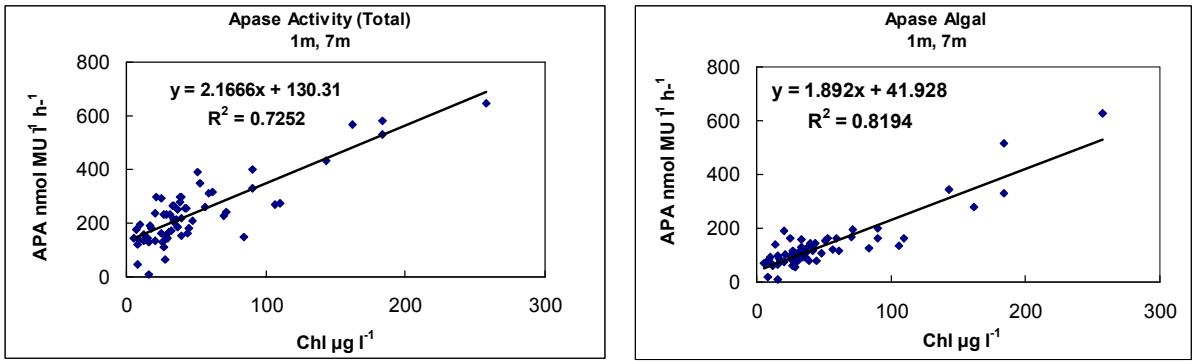

Figure 26: Correlation between chlorophyll and total Apase activity at 1m and 7 m at all stations (left hand panel), and algal activity at 1m, 7m (right hand panel). Data as in Figure 22, but values higher than 300 ug Chl per liter were excluded.

Looking at samples with chlorophyll values above 300 ug Chl per liter, characteristic of a patch, reveal high Apase activity, with high activity in the algal fraction (up to 74%), high community respiration and low conductivity. Surprisingly at these samples soluble reactive phosphorus (SRP) is high in contrast to what was expected, that high alkaline phosphatase activity is a result of low ambient SRP (Table 7).

Table 5: SRP, Community respiration (CR), conductivity, total suspended solids (TSS) and alkaline phosphatase activity (Apase) in samples with chlorophyll values above 300 ug Chl per liter

Station	T	Depth (m)	Chl µg l^{-1}	SRP µg l^{-1}	CR mg O_2 l^{-1} h^{-1}	Cond. ms cm^{-1}	Total Apase nmol $l^{-1}h^{-1}$	Algal Apase nmol l^{-1} h^{-1}	Algal Apase %	Apase nmol µg chl^{-1} h^{-1}	TSS mg l^{-1}
1	T4	1	669	11.89	0.613	0.9368	606.7	448.7	73	0.67	144
10	T4	1	520	6.44	0.404	0.981	390.8	220.3	56	0.42	95.8
1	T5	1	330	7.06		0.9744	573.9	354.7	62	1.07	
1	T7	1	296	6.14		0.9665	313.6	233.2	74	0.79	

These results support the **hypothesis** that in *Peridinium* patches with high biomass and high chlorophyll values, the specific activity per chlorophyll and / or biomass is low, keeping the water in the patch rich in SRP resources, which enables mobilization and attraction of other *Peridinium* cells to join the patch and relief the whole community from phosphate limitation.

Such conditions may enable luxury uptake and further divisions. The low conductivity values within in *Peridinium* patch indicate the contribution of Jordan River water that could be the source of the SRP. Furthermore, besides SRP there may be other "effectors" coming with the Jordan River supplying essential nutrient resources that in the patch are in relatively high concentrations contributing to the patch maintenance.

b. Community respiration and other metabolic activities

We assumed that the spatial distribution of ecosystem variables (e. g.) concentrations of seston or/and chlorophyll under patch formation should follow the pattern shown in Figure 27A, i. e., drastic increase of concentration towards inner areas of the patch itself. The metabolic properties (e.g., primary production or community respiration) along gradient of the mass concentration should be different within and out of the patch (Fig. 27B). We assumed that there should exist a "singular" point (or range) of TSS and Chl concentrations separating and bordering metabolic properties of the patch from areas outside of the patch.

Two experiments were carried out in March and April 2007 in the south part of Kinneret (near Station D). One as part of the *Peridinium* operation and the other one two weeks later.
The following parameters were measured in water samples collected from 1 m depth: Total Suspended Solids (TSS, gravimetrically, after filtering of water samples through GF/F filter); Loss on Ignition at 550˚C; Chlorophyll concentration (Chl, fluorometrically); Community respiration (CR, O_2-method). During experiments in March-April, primary production was measured in parallel with the O_2-method (GPP) and ^{14}C-method (PP). Apparent photosynthetic quotient (PQ) was calculated as PP/GPP (mol C/mol O_2).

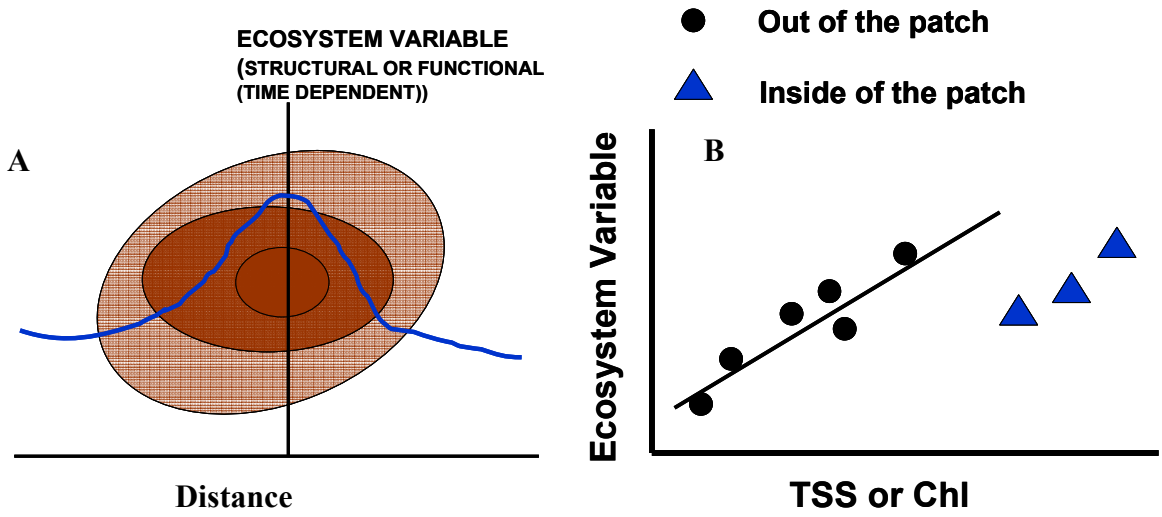

Figure 27: Schematic presentation of spatial distribution of an ecosystem variable and the corresponding concentration along a single transcet across a patch **(A)**; and the hypothetical dependence of a given ecosystem variable (e. g., primary production) on concentration of sesston (TSS) and/or algae (Chl) (B). It is assumed that at higher concentration, this dependence inside of the patch (blue triangles) will be different than outside of the patch (black circles).

Seston concentration (TSS) varied from 2.9 to 144 mg L^{-1} (Figure 28). Very high TSS values (>100 mg/l) were recorded at times T4 and T7 at stations 1 and 10. During the rest of the operation, there were no substantial variations in TSS-dynamics.

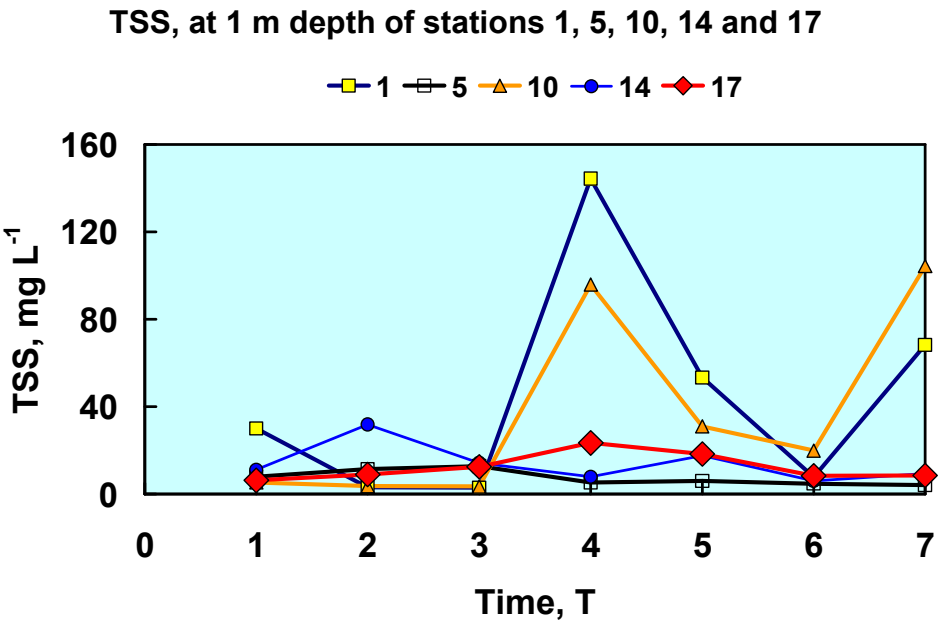

Figure 28: Dynamics of seston concentration (TSS) measured in water samples from 1 m depth

Recorded values of dark community respiration (at times T1 and T4) were proportional to TSS values within the entire measured range of TSS (Figure 29).

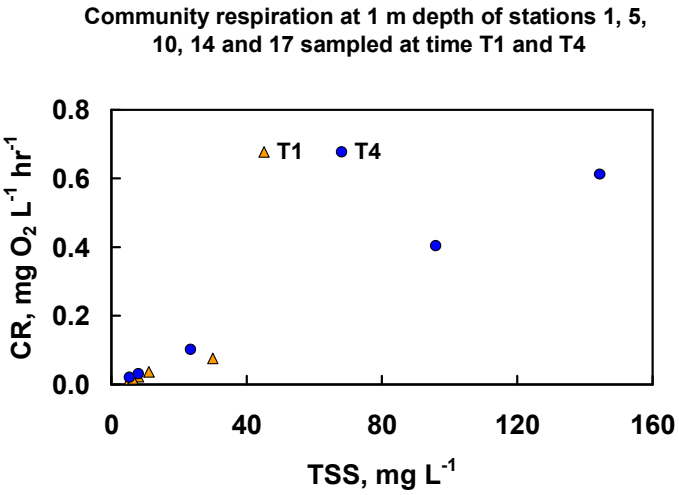

Figure 29: Scatter plot of community respiration (CR) vs seston concentration (TSS) at T1 and at T4.

Community respiration linearly correlated quite well with TSS indicating high constancy (R^2 = 0.95) of TSS-specific respiration within a range spanning two orders of magnitude of TSS, i. e., outside and within the patch (Figure 30).

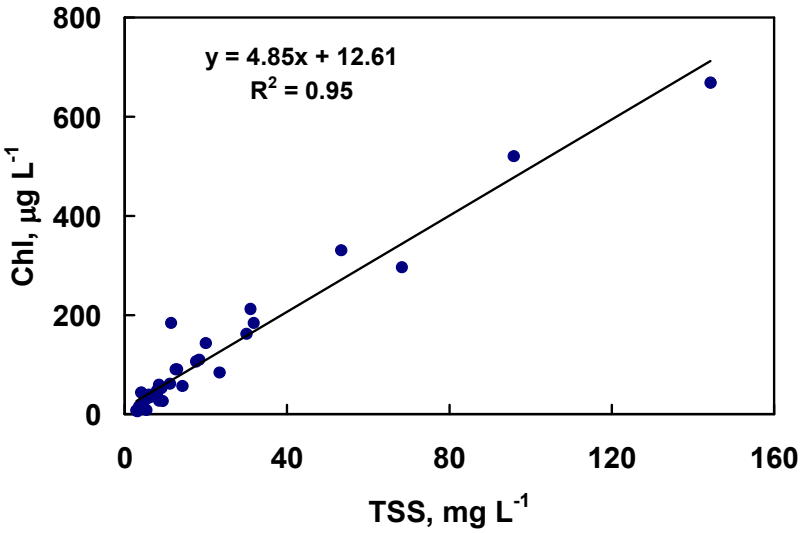

Figure 30: Scatter plot and linear regression for the relationship between CR and TSS.

Combining of the data received on two dates of determinations (in March and April 2007) showed quite well a linear correlation between primary production and community respiration with chlorophyll, in a wide range of Chl concentrations (also spanning two order of magnitude). These data (Figure 31) indicate that the Chl-specific GPP and CR values were similar along a gradient of Chl concentrations (i.e., for water samples from outside and inside of the patch).

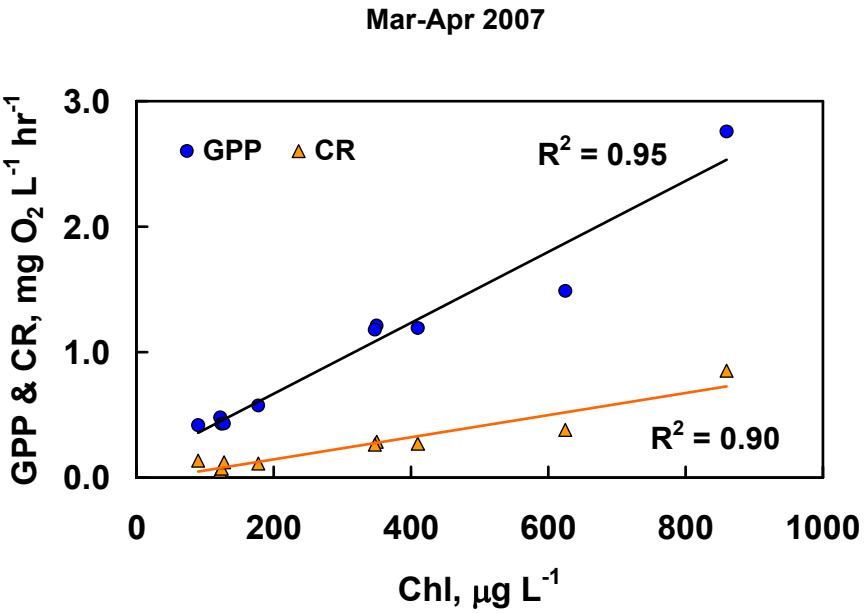

Figure 31: Scatter plots and linear regression between GPP and CR and Chl concentration (data from experiments carried out in March and April 2007 near Station D)

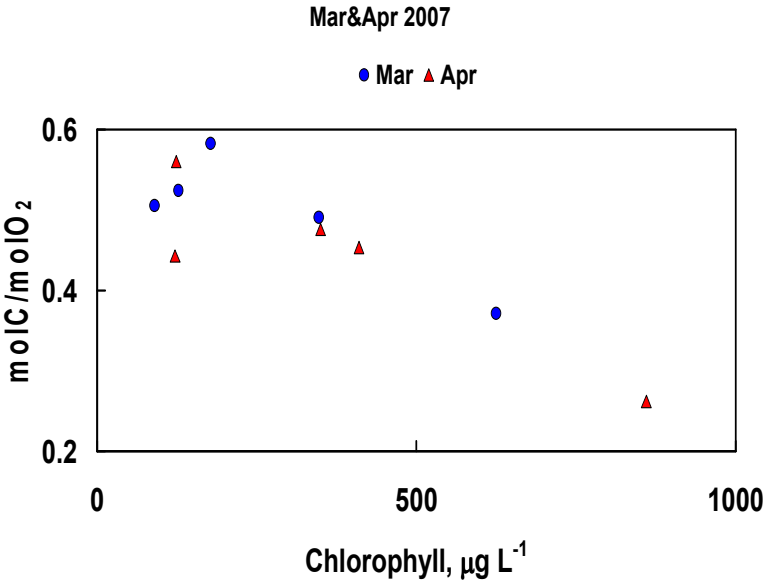

Figure 32: Scatter plot of the relationship between the apparent photosynthetic quotient and chlorophyll concentration obtained from the experiments carried out in March (circles) and April (triangles) 2007 in south part of Kinneret

The data obtained from the experimental series carried out in March-April 2007 indicated that for concentrations of Chl>150 µg L^{-1} there was a gradual drop of the apparent photosynthetic quotient (PQ = PP/GPP) as presented in Figure 32. We have no explanation to this tendency, though it should be noted that calculated PQ were well below of those published in literature.

Based on the relationships between ecosystem variables including seston and chlorophyll concentrations, primary production of plankton and community respiration during *Peridinium* bloom in Lake Kinneret in May-April 2007, we conclude that there were no significant differences in seston and chlorophyll specific values of primary production and community respiration obtained for areas inside and outside of the *Peridinium* patches.

Selected set of variables and relationships among them did not allow us to confirm the working hypothesis about existence of the metabolic differences and associated ecological "benefits" in formation of the *Peridinium* patches.

7. Distribution and spatial variations of Chemical parameters (Ami Nishri)

a. Electrical Conductivity and other geochemical parameters

It is clear that the area designated in Lake Kinneret (LK) for the patchiness experiment is directly affected by inflows from the Jordan River. The river water are characterized by a significantly lower electrical conductivity (roughly 600 µS/cm) as compared to LK water (~1050 µS/cm). This difference is used to trace Jordan River water within LK water. However there are some limitations to this approach.

Electrical conductivity (EC) measurements (normalized to 25°C) are affected by the concentration of ions in solution. Divalent ions carry more "electricity" than mono-valent ions, hence 1mM mono-valent ion (such as Cl^- or Na^+) will have smaller EC as compared to an identical concentration (in molar terms) of a divalent ion (for instance Ca^{+2}). As will be shown below in some cases EC measured in LK may be affected by the removal of Ca^{+2} and CO_3^{-2} ions through the precipitation of calcite. Thus EC by itself should be treated cautiously, particularly since the patchiness experiment took place further away from the Jordan River mouth, where most of the surface reduction in EC would probably be due to calcite sedimentation or later during the bloom period where calcite sedimentation flux is larger.

EC measurement by itself is a very accurate, reproducible and easy to measure parameter (Error in the order of 0.2-0.3%). The reasons for the large difference in EC between the river and the lake water are that the Jordan River contains much less Cl^- (~10 mg/l) and Na^+ (~12 mg/l) and some other major ion solutes as compared to Lake Kinneret water. However the Jordan River contains a slightly higher alkalinity (~180 mg$CaCO_3$/l) and Ca (~65 mg/l) then LK epilimnion (<120,<50 mg/l, respectively). Mixing of Jordan River water with Lake Kinneret water brings about a reduction in EC because of the predominant effect of Na, Cl, Mg and SO_4 on the overall EC measured. However one would expect that the mixture would contain slightly higher alkalinity and Ca, provided that no calcite sedimentation took place from this mixture.

The large difference in concentration between Cl^- (and sometimes of NO_3^-) in the river to that of Lake Kinneret makes it a more precise tool to determine the extent of mixing of river water, within the lake. However using Cl^- to trace the dilution requires in-lab analysis. In Lake Kinneret, one should also be aware of the possibility that submerged brackish springs may cause local elevated Cl^- (and EC) levels. Thus unless close to submerged saline water seepages, Cl content, relative to Lake Kinneret average should give an accurate measure of Jordan River dilution effect. The same is true also for NO_3 that in some cases can be considered as a conservative solute (to be discussed below). If the dilution factor obtained through Cl^- budget is identical to that obtained from NO_3 budgeting it is possible to claim that neither saline sources nor NO_3 biological removal/addition (algal consumption, denitrification, nitrification) are affecting the data and that the dilution factor obtained is accurate. In the following discussion it will be shown that this was the case in the March 2007 experiment.

During the course of the March 2007 *Peridinium* patch experiment we did not collect water samples from Jordan River. Thus, no data was available for Cl^- or NO_3^- levels in the river and the solving of the dilution factor was not a straight forward issue. However contrary to NO_3, in spring Cl^- levels in the river vary very little, thus one may assume a concentration of 12 mgCl/l. Nitrate however varies considerably, depending on river water discharge and water flushing through the soils in Hula Valley. River Jordan dilution percentage (X%) calculated here through Cl^- concentration using the following formula:

$$X\ \% = [(245-[Cl_{mes}].)/233)]*100$$

where 245 mg/l represents Cl^- concentration in "pure" Lake Kinneret water and 12 mgCl/l is the concentration of Cl^- in Jordan River water (hence 233 = 245-12). $[Cl_{mes}]$ stands for the measured Cl^- concentration in the sample. Using this equation the putative percentage Jordan River water in the analyzed Lake Kinneret water was calculated for samples collected from various stations and depths during the *Peridinium* operation (Table 6). The calculated values are presented in Table 6 together with the corresponding chlorophyll concentrations in order to indicate samples with high *Peridinium* concentration (labeled by yellow background).

Table 6: Calculated values on the putative Jordan River water percentage in Lake Kinneret water samples presented together with the corresponding chlorophyll concentrations for different sampling sites and times.

Cruise number	Station	Chlorophyll ug/l 1m	Chlorophyll ug/l 7m	Cl mg/l 1m	Cl mg/l 7m	Jordan Water % 1m	Jordan Water % 7m
T1	1	162	10	234	241	5.5	2.6
T1	5	38	33	244	243	1.3	1.7
T1	10	32	17	241	242	2.6	2.1
T1	14	61	56	243	242	1.7	2.1
T1	17	36	34	240	239	3.0	3.4
T2	1	6	9	237	239	4.3	3.4
T2	5	184	32	242	244	2.1	1.3
T2	10	12	12	237	237	4.3	4.3
T2	14	184	51	241	240	2.6	3.0
T2	17	53	37	240	238	3.0	3.8
T3	1	8	8	237	237	4.3	4.3
T3	5	91	18	245	243	0.9	1.7
T3	10	16	16	237	236	4.3	4.7
T3	14	57	20	242	241	2.1	2.6
T3	17	90	39	238	233	3.8	6.0
T4	1	669	70	225	210	9.4	15.7
T4	5	8	25	243	245	1.7	0.9
T4	10	520	45	235	228	5.1	8.1
T4	14	48	26	240	242	3.0	2.1
T4	17	84	30	241	234	2.6	5.5
T5	1	330	17	230	232	7.2	6.4
T5	5	39	31	243	243	1.7	1.7
T5	10	212	21	226	231	8.9	6.8
T5	14	106	39	233	242	6.0	2.1
T5	17	110	71	234	239	5.5	3.4
T6	1	42	40	230	230	7.2	7.2
T6	5	27	29	243	243	1.7	1.7
T6	10	143	43	235	236	5.1	4.7
T6	14	34	25	242	244	2.1	1.3
T6	17	59	29	242	245	2.1	0.9
T7	1	296	36	226	236	8.9	4.7
T7	5	44	14	244	244	1.3	1.3
T7	10	257	34	214	242	14.0	2.1
T7	14	27	15	245	243	0.9	1.7

*The values marked in yellow are : a. exceptionally high Chl values, b. Low Cl values and c. high percentage of Jordan River water in Lake Kinneret (> 4.5%). Estimated error for the dilution factor is ~1%.

The plot of chlorophyll levels against the percentage of Jordan River water (Figure 30) shows a weak positive correlation. This suggests that the river mouth is an important source of chlorophyll but that other processes are also involved. One such possible process is the vertical migration of algae within a plume of river water. The correlation between Chl and the respective percentage of Jordan River water in the 7 m depth layer is worse (R^2=0.17: not shown).

It is further assumed that the extremely high percentage of river water in the sample withdrawn from station 1 at T4 (7 m depth = 15.2%) should be treated as an indication for a direct massive flow of Jordan River water, and therefore for this plume NO_3 may be treated as conservative solutes, as only an insignificant portion of the original river NO_3 may have been consumed in this sample. It thus became possible to calculate the concentration of nitrate in the river, as following. Nitrate average concentration in Lake Kinneret is assumed to be 0.199 mgN-NO_3/l

(see relevant data); a dilution of 15.2% was introduced into the Cl type formula but this time using NO_3 data. From this calculation it was estimated that Jordan River NO_3 concentration should have been 1.78 mgN/l. This is a reasonable concentration for this period of the year. Once river levels are known it was possible to calculate the percentage of river water in the samples, but this time using measured NO_3 data instead of chloride. The correlation between percentages of dilution according to Cl Vs. NO_3 is shown in Figure 34, suggesting that both tracers lead to similar dilution.

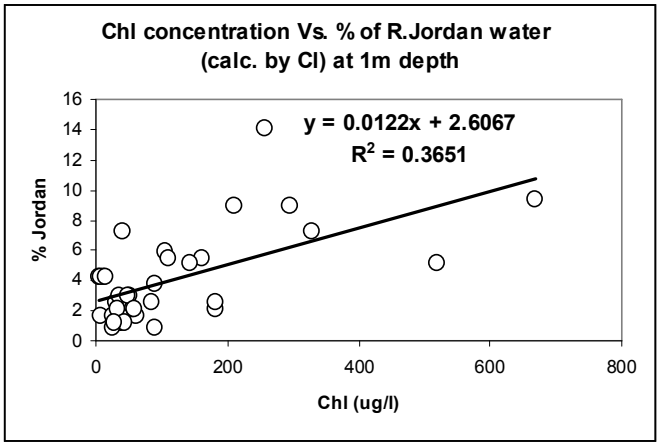

Figure 33: Chlorophyll concentration Vs. % of Jordan River water in Lake Kinneret water samples collected from 1m depth during the *Peridinium* operation experiment.

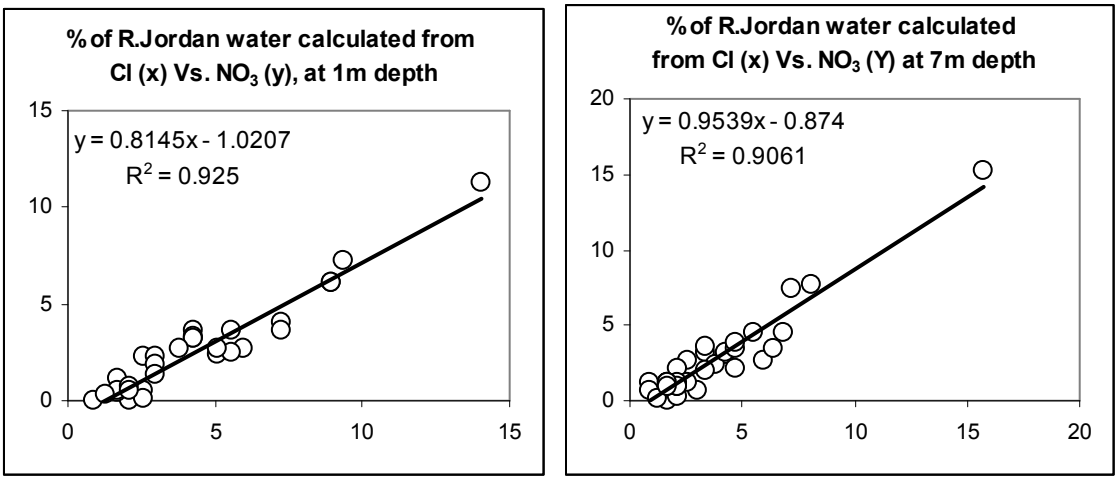

Figure 34: Correlation between the dilution estimated through Cl to that estimated through NO3 at 1m depth (left) and 7m depth (right).

A point of interest is that during its transport from the river mouth to the area where sampling took place NO_3 behaves like a conservative solute and its vertical concentration profile is in accordance with its relative sources. In other words having higher or lower (NO_3) at a certain depth is related to the percentage of Jordan River water. Unlike nitrate, NO_2 had relatively stable concentrations, at ca.0.03 mgN/l, independent of the presence of Jordan River plumes. Ammonium concentrations in all of the samples were low, mostly below 10 μgN/l.

As suggested above, EC may be affected by calcite precipitation as well. A rough idea on how much calcite is precipitated from a water sample can be obtained by comparing alkalinity (or Ca) data at 1m depth to that of 7 m depth, taken on the same profile. We prefer alkalinity data as we have a relatively low analytical error (<0.7%). The relevant data for different water sampling stations are presented in Figure 35 for the 1m and 7m depth layers (for T7 a 10 m layer is shown rather than 7 m layer).

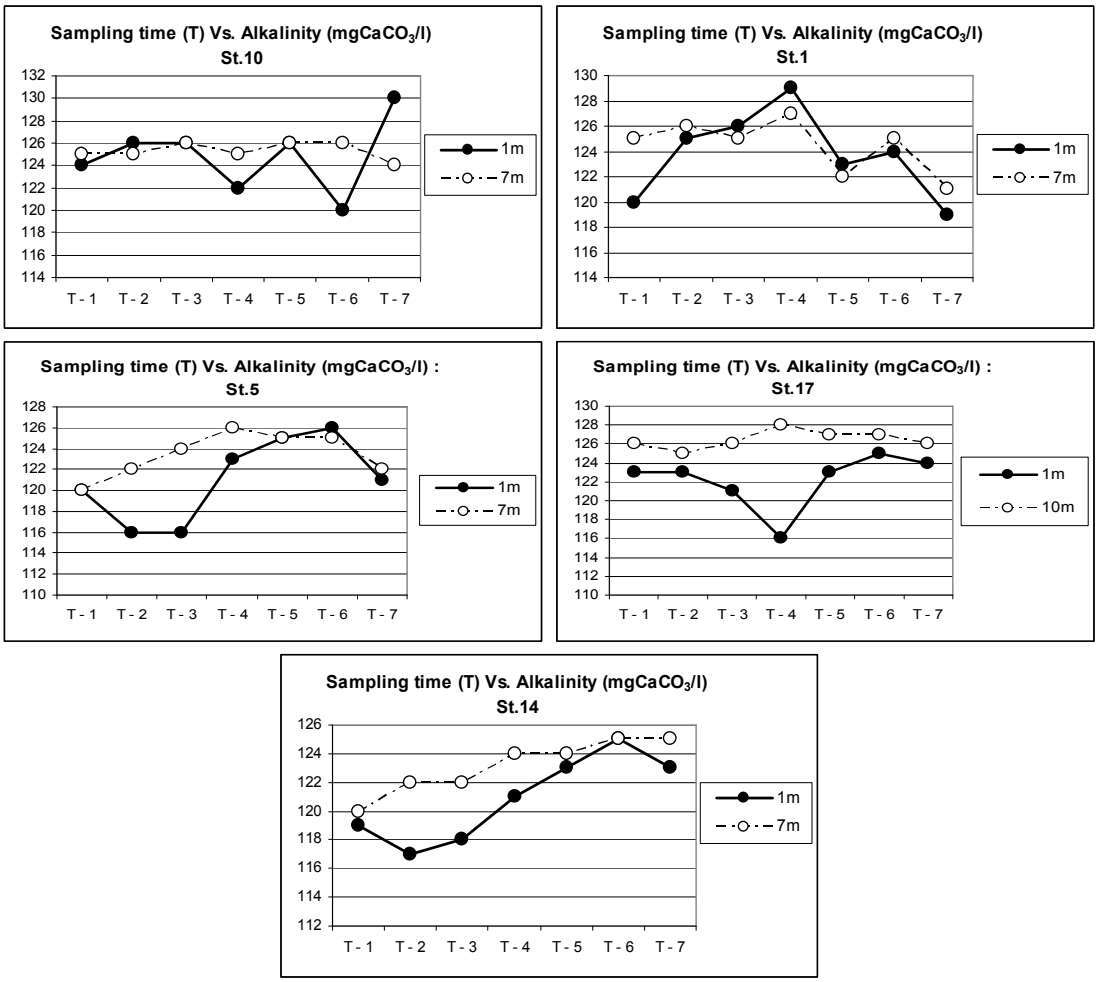

Figure 35: spatial/temporal/depth variations in alkalinity during the Peridinium operation. Data presented separately for each sampling stations. For stations 1, 5, 10 and 14 the data is presented for the 1 m and 7 m depth while Stn. 17 the data is presented for the 1m and 10m depths.

In most cases the alkalinity pattern shows lower levels in the upper water layer (1m depth). This is caused by autochthonous calcite precipitation in this layer which is characterized by higher productivity. Since most of the productivity occurs within the upper 4 m layer $CaCO_3$ precipitation is expected to occur only within this layer. Thus as long as sluggish vertical turbulence prevails, a clear differentiation in Alkalinity (and EC) is expected to prevail between the upper most layer and the layers below. In the deeper layers, below the euphotic zone, alkalinity is not expected to correlate with algal biomass. From the thermodynamic point of view (saturation index) calcite precipitation may also take place at the Jordan River mouth, upon emerging to the lake. During the *Peridinium* experiment there were several cases where surface water (1 m depth) samples that contain a high number of algal cells show alkalinity deficiency, part of which may be attributed to $CaCO_3$ deposition.

Deeper layers preserve higher levels of alkalinity (and of Ca). In the lowest layer examined here (St. 17, 15m depth, not shown) the alkalinity is even higher, at ca. 130 mg ($CaCO_3$/l). This could be a result of partial dissolution of some calcite there.

b. Hydrolab data

Here we present and discuss several data sets from the Hydrolab profiles acquired during the operation. The temperature profile obtained in T4 station 1 (10:59 am) of March 23rd, 2007 reveals the daily heating of the upper most water layers (0 - 1m depth - Figure 33 left), Electrical conductivity (EC) profile (Figure 33 right) suggests that the entire upper 8m layer is diluted by Jordan River water. "Pure" Lake Kinneret water would have a conductivity of 1.028 mS/cm (vertical filled squares in Figure 36).

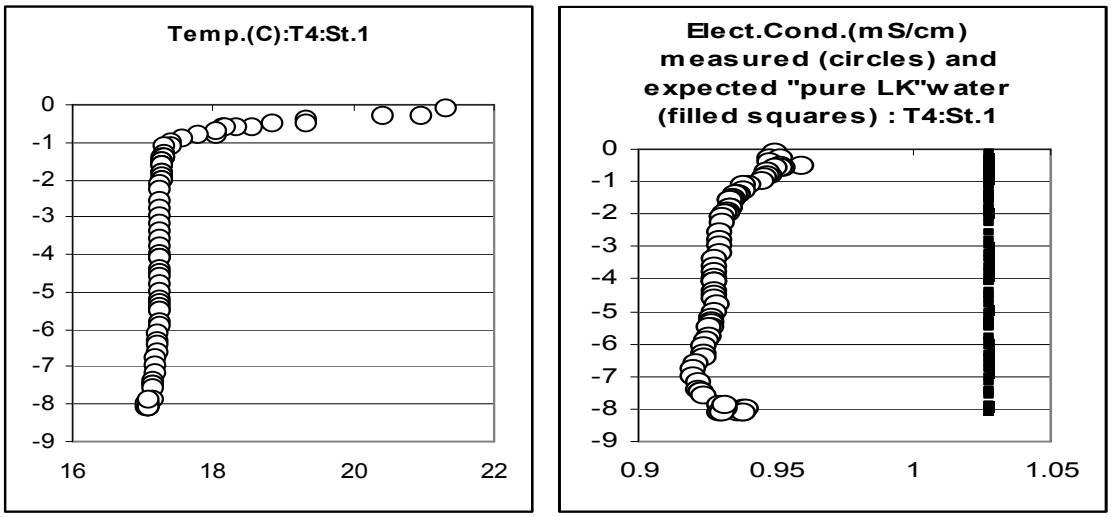

Figure 36: Temperature profile (left) and Electrical conductivity (EC) profile (right) measured in Station 1 at T4.

Dilution by Jordan River water (by the NO_3-Cl method -see above) accounts for 15.2% of the water in the 7 m horizon (Table 6) while in the 1m horizon, the respective dilution is only 6.7%. The chlorophyll maxima depth (surrogated in our case by the turbidity profile) appears to be concentrated with in the upper 1m layer, having a prominent peak at 0.5 m. The respective DO profile (Figure 37) also shows prominent maxima at 0.5 m depth, where DO production minus diffusion to the air (atmosphere) above and to the underlying water is largest. These findings suggest that the 0.5 m depth layer is also where maximum primary productivity (PP) occurs. The respective pH profile (Figure 38), however does not show a peak at 0.5 m depth but rather a continuous increase toward the water-air interface. This implies that CO_2 (aq) concentration at the top most layer is lowest and that the air above does not provide CO_2 for the 0.5 m depth maximum PP layer. Assuming that for PP *in Peridinium* cells may consume only CO_2 (aq) there are only two potential sources of it to the PP maximum layer. One is diffusion from below and the other one is calcite formation, which releases CO_2. Alkalinity data (Figure 35) shows a concentration of ca. 128 mg$CaCO_3$/l at 1m depth, and that the 7m and 1m layer have similar alkalinities. Hence at this stage $CaCO_3$(s) formation can not be a source of CO_2 to the maximum PP layer. The only potential source left is diffusion from the layer below, which is expected to be relatively small. Therefore the *Peridinium* growth is possibly limited by CO_2 availability. (Note that a paper summarizing these issues is now under preparation).

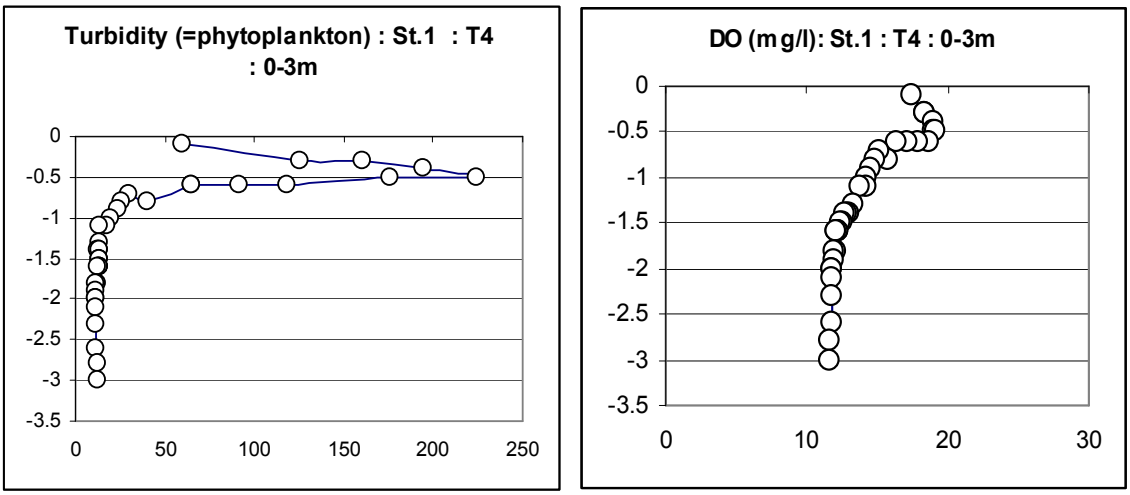

Figure 37: Turbidity (surrogate for algal biomass) profile (left) and DO profile (right) measured in Station 1 at T4.

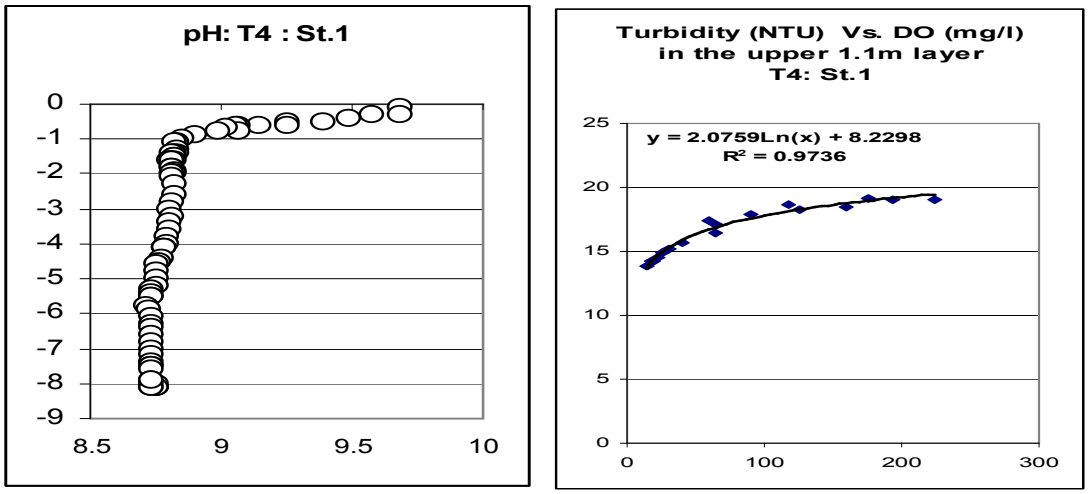

Figure 38: pH profile (left) and the relationships between turbidity and DO (right) as measured in station 1 at T4.

Despite of the distinguished Jordan River water signal that penetrates the water column down to 5–7 m depth the *Peridinium* population is found mostly within the upper 1 m layer during morning hours where PP takes place. This supports previous observations (Pollingher and others) that in Lake Kinneret the *Peridinium* maintain their vertical position in accordance with ambient light conditions and possibly other unknown factors.

An additional example of the dynamics of various geochemical parameters is provided by the Hydrolab data obtained at Station 14 at T7. The onset of seasonal thermal stratification can be seen as a minor temperature gradient (thermocline) was recorded at ca. 15 m depth. This profile is also characterized by an increase in EC with depth (Figure 39). The later is due to some $CaCO_3$ removal from the upper water mass and perhaps partial dissolution in the lower layers. Turbidity profile (Figure 40) shows a prominent peak in the upper 2 m layer and a secondary peak at 5m depth. Both DO and pH profiles reflect the occurrence of enhanced PP in the upper 2 m layer.

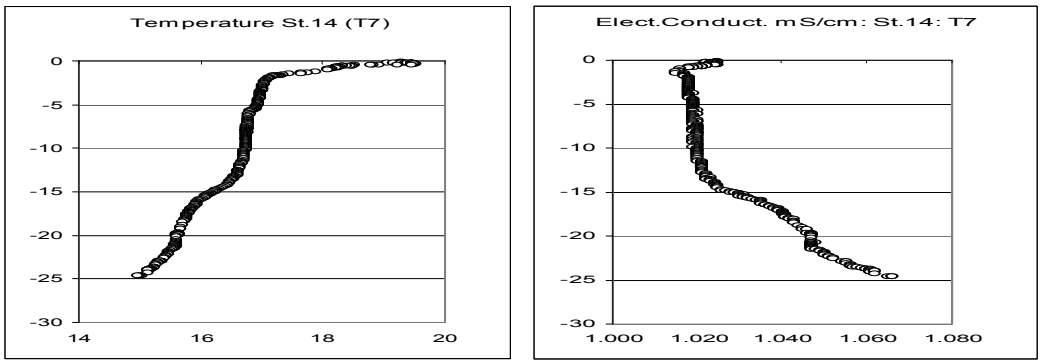

Figure 39: Temperature profile (left) and EC profile (right) measured in Station 14 at T7

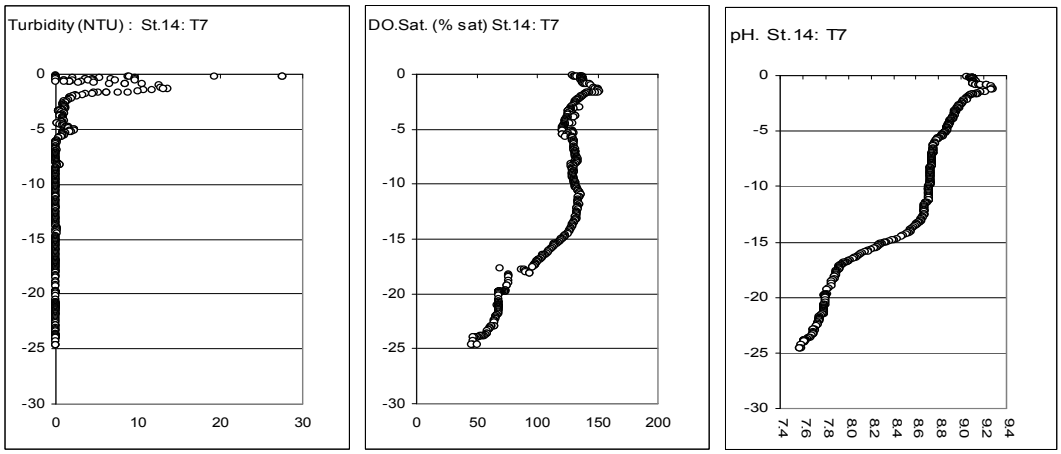

Figure 40: Turbidity (surrogate for algal biomass) profile (left), DO profile (center) and pH profile (right) measured in Station 14 at T7.

Zooming on the upper 7 m layer (Figure 41) it is possible it to note that the turbidity peak (algae) is located at 1.3 m depth and that an additional somewhat smaller turbidity peak is detected within the upper 1m layer. Similar phenomenon can be seen for DO and pH profiles. Thus it is speculated that on that early afternoon hour (13:00 pm) local algae were already moving downward leaving behind (above) slightly DO enriched and CO_2 depleted (higher pH) water layer. An additional phenomenon that can be observed in that data set is the minor change in conductivity, from 1018 to 1025 μS/cm (~0.7 ‰) at the upper 1 m layer (Figure 42). If turbulence may be ignored, this observation suggests an evaporation of ca. 6 mm during the morning hours of March 26th.

The same data set (Station 14 T7) shows an additional minor peak of turbidity at 5m depth layer, just above a small step like decrease in temperature (Figure 41). This stratum is also characterized by DO deficiency (Figure 41) suggesting net DO removal, probably due to respiration. These observations of turbidity accumulation above the temperature step suggest that the lower boundary of *Peridinium* migration is somehow linked to "physical barriers".

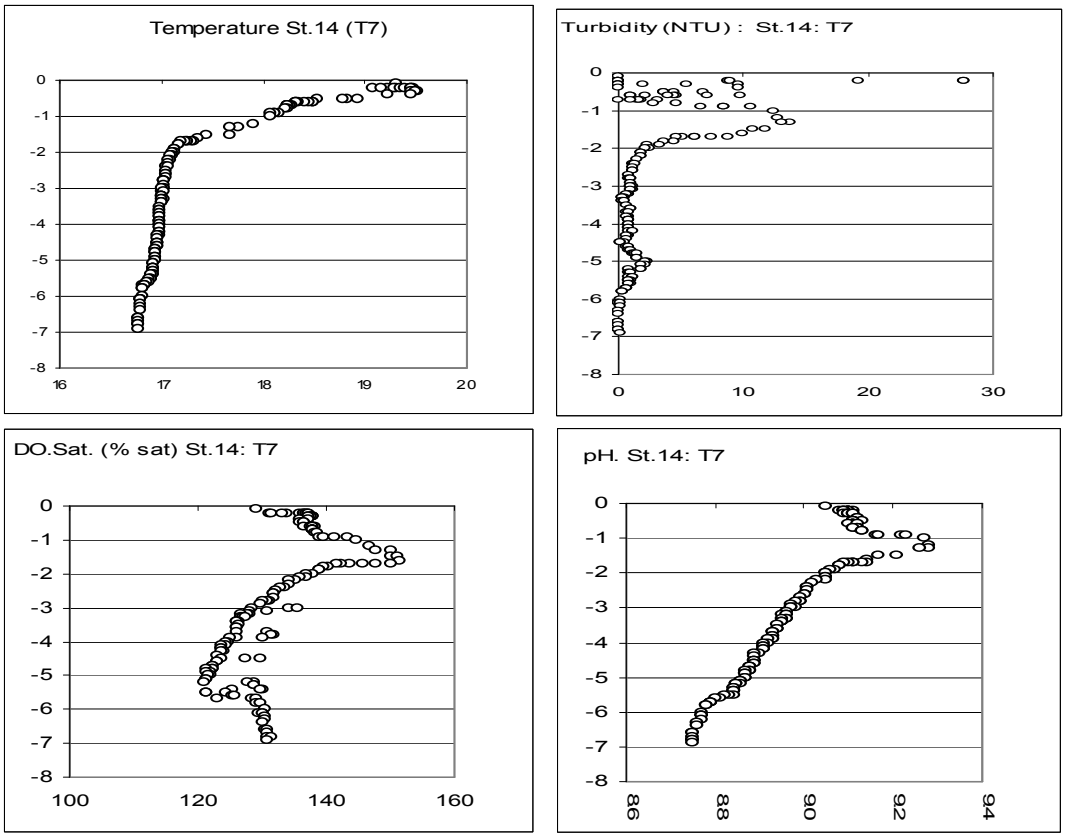

Figure 41: Hydrolab data. St.14 : T7, upper 7m: temperature (up left) and turbidity (up- right). DO (low left) and pH (Low-right)

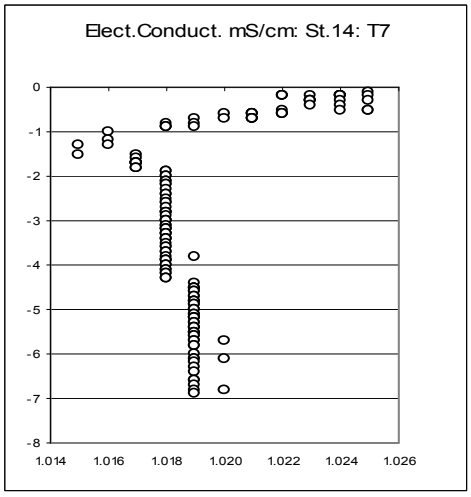

Figure 42: Vertical variations in electrical conductivity in the 0-7m depth water layer in station 14 at T7.

8. Wind field, water circulation, and transport of soluble material (Alon Rimmer, Elad Shilo)

Introduction

Water movements play a key roll in mixing and transport processes at the lake. Heat, nutrients, soluble and particular materials are mixed through the water column. The environmental factors that forced the lake during this time of winter (e.g. wind field and inflows of the Jordan River and other streams) markedly differ from those during summer. In the present study, the water movements during the end of March 2007, was investigated using state-of-the-art three-dimensional (3-D) hydrodynamic model ROMS (Regional Ocean Modeling System). The model was forced by interpolated wind fields, using observations from four meteorological stations.

The numerical model

ROMS is a free-surface hydrostatic, primitive equation ocean model that uses stretched, terrain-following coordinates in the vertical and orthogonal curvilinear coordinates in the horizontal. In the vertical, the primitive equations are discredited over variable topography using stretched terrain-following coordinates (Song and Haidvogel, 1994). The stretched coordinates allow increased resolution in areas of interest, such as thermocline, bottom and surface boundary layers. There are several subgrid-scale parameterizations in ROMS. Horizontal mixing of tracers and momentum can be along vertical levels, geopotential (constant depth) surfaces, or isopycnic (constant density) surfaces. The mixing operator can be harmonic or bi-harmonic. The vertical mixing parameterization in ROMS can be either by local (2.5 level turbulent kinetic energy equations by Mellor and Yamada, 1982), or non-local closure schemes K-profile, boundary layer formulation by Large et al. (1994). Air-sea interaction boundary layer is included in ROMS, based on the bulk parameterization of Liu et al. (1979) and Fairall et al. (1996). It allows the computation of surface fluxes of momentum, sensible heat, and latent heat. The model was adapted for use in Lake Kinneret. It was and verified especially for winter currents during the work of Shilo et al. (2007).

Calculating wind fields above the lake using wind measurements

The Cressman (1959) method was applied to calculate the wind field over the water surface of the lake. According to this method the components of the wind velocity vector at a certain grid point are calculated as a weighted average of the wind in measured points. In the results of the Cressman method the requirement for mass conservation for the 2D wind field is not met, and therefore the method of Brocchini et al. (1995) was applied in order to minimize the divergence of the interpolated 2D wind field.

The proposed algorithm was applied to the wind measurements from 4 permanent meteorological stations, located on and off shore Lake Kinneret (station A (TA), Tabgha (MT), Bet Zeida (BZ) and Tzemach (TZ), (Figure 43). The stations measure simultaneously, every 10 min, the following meteorological variables: Air temperature, relative humidity, wind speed and direction, and short and long wave radiation. In TA and MT the water surface temperature is measured as well.

Model run

The objective of this run was to gain a preliminary knowledge about the current field in Lake Kinneret during the experiment of March 2007. The scenario we ran was subject to the following details:

Time interval: 10 days, starting from the 22.03.2007 00:00 local time.

Surface forcing: Wind fields, calculated from four meteorological stations.

Jordan River inflow: 27 m^3 sec^{-1}

Tracer: Starting at 24.03.2007 00:00 (hour 48 in the hydrodynamic model) a one hour pulse of passive tracer was introduced in the entrance of the Jordan River. The initial concentration was 1 PSU**.**

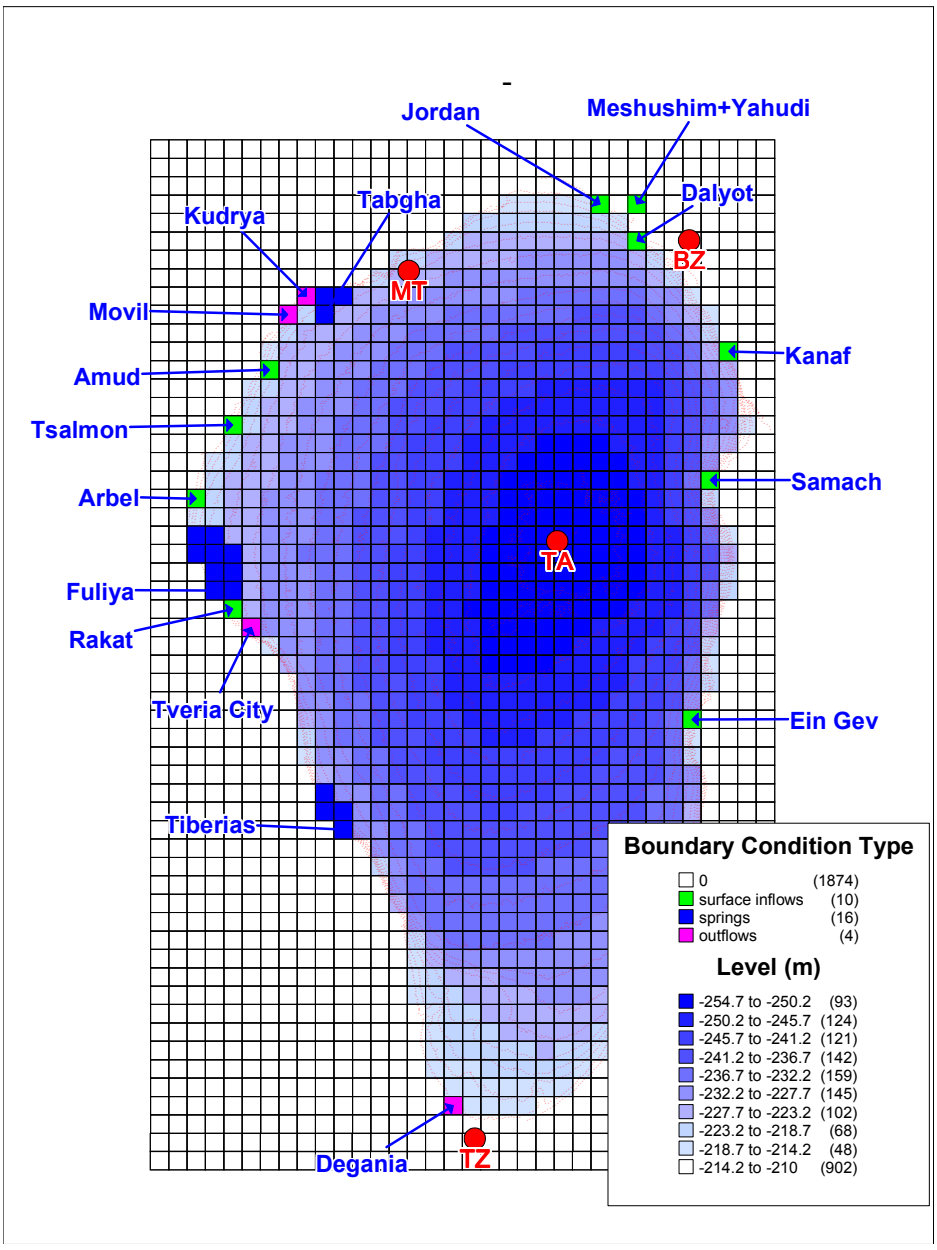

Figure 43: Structure of the ROMS grid which was applied in the model. The boundary conditions which were applied during the March 2007 experiment were the Jordan River inflows and the wind field calculations based on measurements from Tabgha (MT), Bet Zeida (BZ), Zemach (TZ), and A (TA) meteorological stations.

Observations

Current observations: Vertical profiles of horizontal current velocities were measured using 300 kHz ADCP (Teledyne RD Instruments) located at two different points. One ADCP was located at the deepest part of the lake (Station A, Figure 43), and measured currents speed and direction

in depth of 3.2 to 36.2 m' with a depth interval of 1 m'. The second ADCP was located at shallower area not far from the MT Station (Figure 43), and measured the currents in depth 1.9 to 13.9 m with a depth interval of 0.5 m. The ADCP Current velocities were sampled at 0.1 Hz frequency and averaged over ten minutes interval. A typical current measurement is shown in Figure 44.

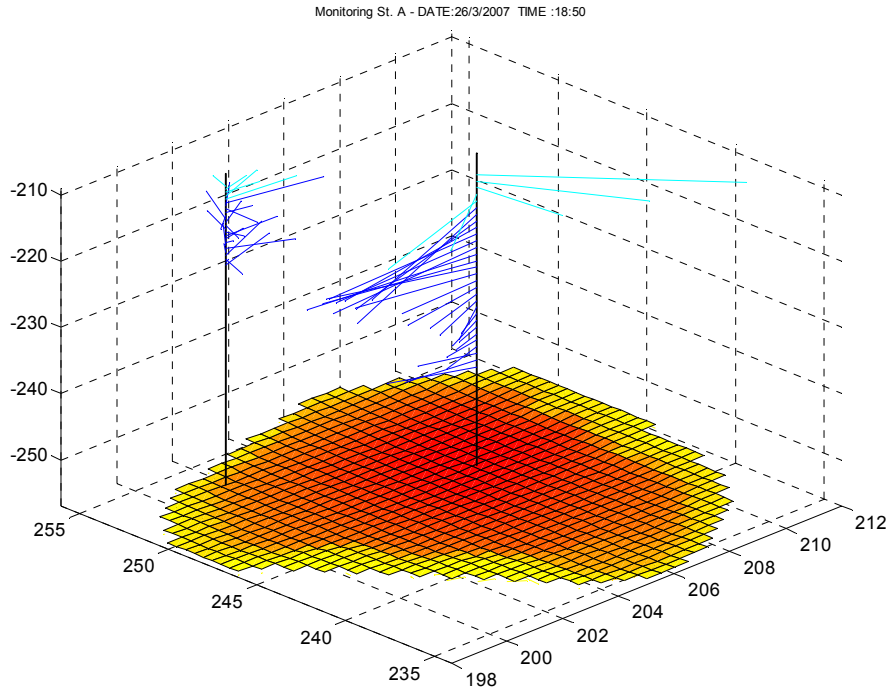

Figure 44: Example of current measurements from Station A and Tabgha. The current speed and direction are indicated by the length and direction of the lines respectively. The upper line in Station A is the current vector at depth 3.2 m', with speed of 6 cm/sec in the direction of 144^{o}.

Meteorological observations: In all stations, measurements of wind speed (m s^{-1}) and wind direction (degrees) were taken by a YOUNG wind monitor MA-05106, located 10 m' above ground level (BZ, TZ), and 6 m' above the water surface (TA, MT). Measurements were taken each second and averaged over 10 minutes interval. Later, for the purpose of modeling the data were converted to the east-west (U), and the north-south (V) components, and were averaged over one hour period (Figure 45).

Temperature observations: In addition to the temperature profiles which were sampled during the experimental procedure, temperature measurements (three profiles in a minute) were taken with an LDS system. The LDS consist of a CWR Thermistor Chain, which is a single cable thermistor chain with up to 40 thermistors at user-specified intervals along the one cable. In Lake Kinneret the interval between termistors is 0.75 m depth. The LDS measurements provided an excellent data on the structure of the temperature profile. An additional information on the lake temperature was provided by a commercially made water column profiling unit (Remote Underwater Sampling Station, RUSS, Apprise Technologies), which was operated on a "ecological monitoring raft". The RUSS is equipped with a set of YSI probes, capable of automatically in-situ monitoring of depth, temperature, conductivity, dissolved oxygen, pH, chlorophyll fluorescence and turbidity. It is usually programmed to conduct 4 profiles daily at 2 m depth intervals between 3 – 39 m.

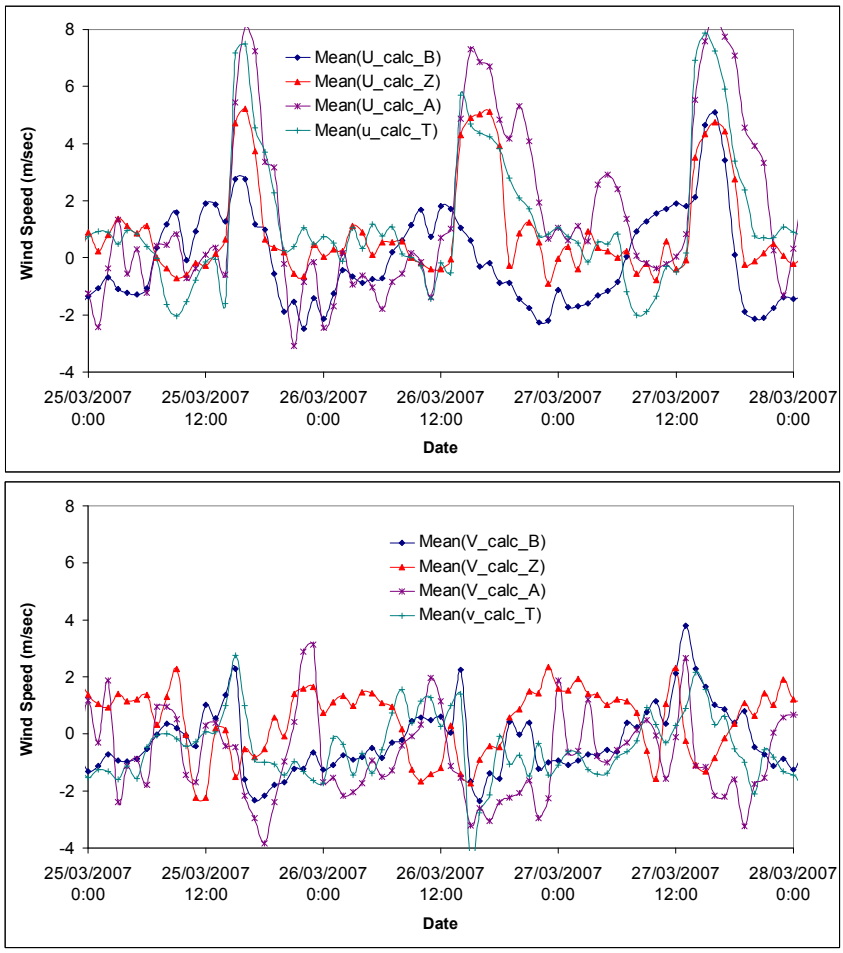

Figure 45: Hourly averaged wind measurements from Tabgha (MT), Bet Zeida (BZ), Zemach (TZ), and Station A (TA) meteorological stations. Top: The East-West average hourly component. Low: The North-South component

Results and discussion

The hydrodynamic model was operated according to the input data 4 days before the actual experiment was started. The initial vertical temperature profile was provided using a simple equation of lake stratification (Rimmer et al. 2005). Boundary conditions, including wind field, air temperature and radiation were provided from the meteorological stations for the next 10 days on an hourly basis. Model typical temperature profiles of the lake were similar to the measured profiles (Figure 46), which indicated the first stages of thermal stratification, with the thermocline at nearly 10 m depth.

Continuous analysis of the measured currents in Station A indicated that the currents speed fluctuated in the range of 1-8 cm/sec, depending on the time and depth of measurements. Direction of the currents in the center of the lake changed in clockwise direction. Comparison between the diurnal cycle of measured and modeled currents in Station A (Figure 47) resulted in a reasonable agreement. The same analysis for the measured currents near Tabgha resulted in lower speed but did not result in clear understanding of "typical" currents direction. The full picture of lake wide currents speed and direction, for the average flow in 0-8 m' depth (Figure 48) reveals an obvious flow from the Jordan River inflow towards Tabgha, during the entire period of 25-28 of March.

Farther confirmation for this understanding was achieved with the virtual passive tracer movement, shown for 0, 24, 48 and 72 hours (Figure 49), and 96, 120, 144 and 168 hours (Figure 50). Note that the 0 hours Figure illustrates the initial condition at 24.03.2007 00:00 local time, 48 hours after the beginning of the model run, when the tracer was introduced in the entrance of the Jordan River for 1 hour with an initial concentration of 1 PSU**.** The dispersion of the tracer is expressed as an average concentration over the entire lake depth. The illustrations describes an obvious movement of the tracer to the south-west (Tabgha direction) for the first 4 days, followed by a move to the south, and later towards the center of the lake. These preliminary calculated flow directions are in agreement with the general hypothesis that lake mixed Jordan River water act as a major components of *Peridinium* patchiness development. It should be noted however, that a further work to identify the dynamics of the Jordan River and other streams in the lake is needed.

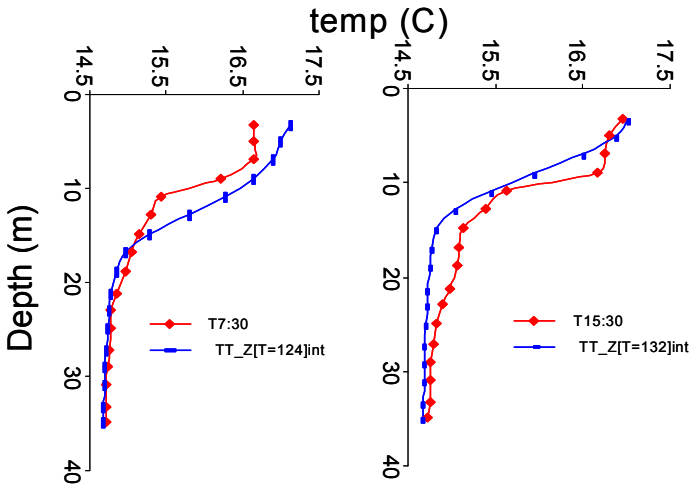

Figure 46: Typical temperature profiles of the lake (red-measured; blue-modeled) during the March experiment.

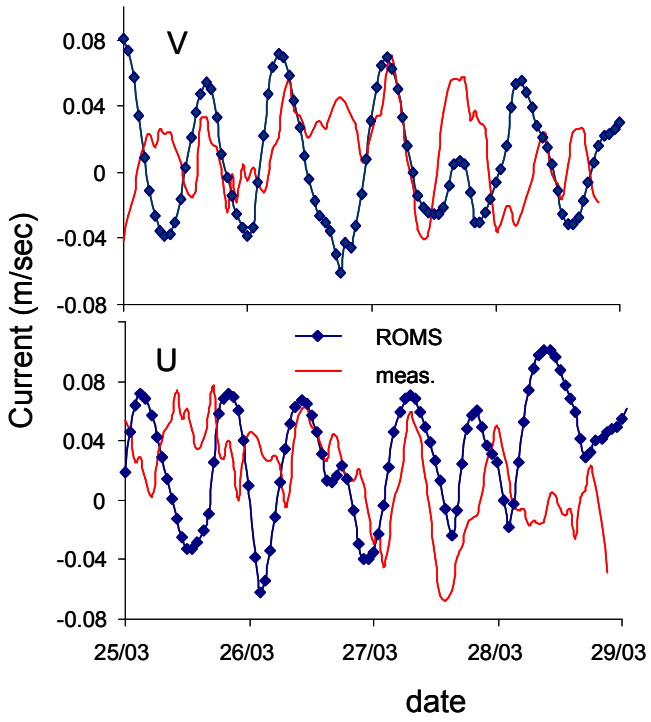

Figure 47: Comparison of measured (red) and model (blue) components of currents in the upper 8 m in Station A during 25-29/3.

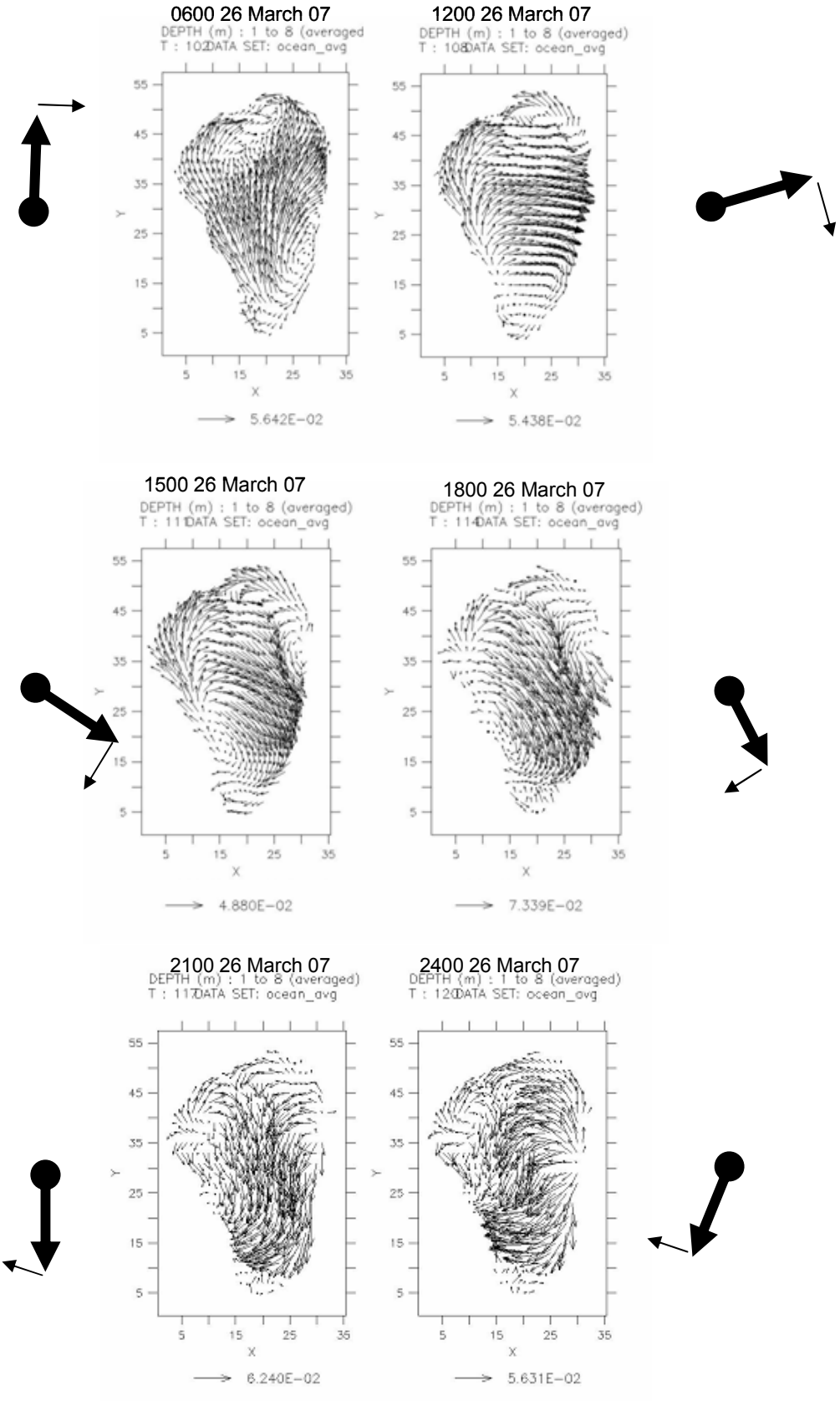

Figure 48: Current directions during the 26/3. In the center of the lake current direction (large arrows) changed in clockwise direction (small arrows). In the north of the lake an obvious flow from the Jordan River inflow towards Tabgha was calculated.

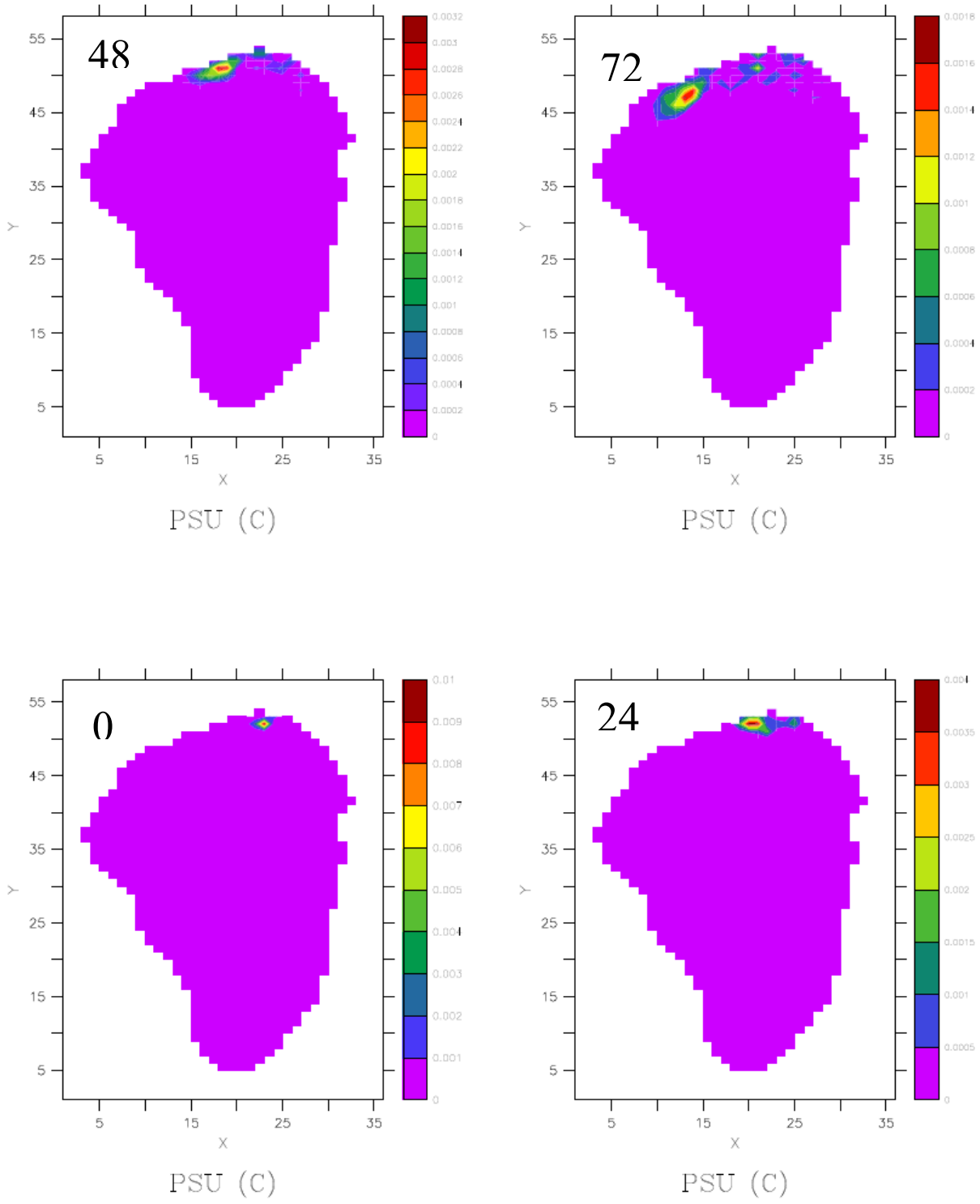

Figure 49: Tracer dispersion in the lake 0, 24, 48 and 72 hours after the tracer was introduced in its initial location at the Jordan River inflow.

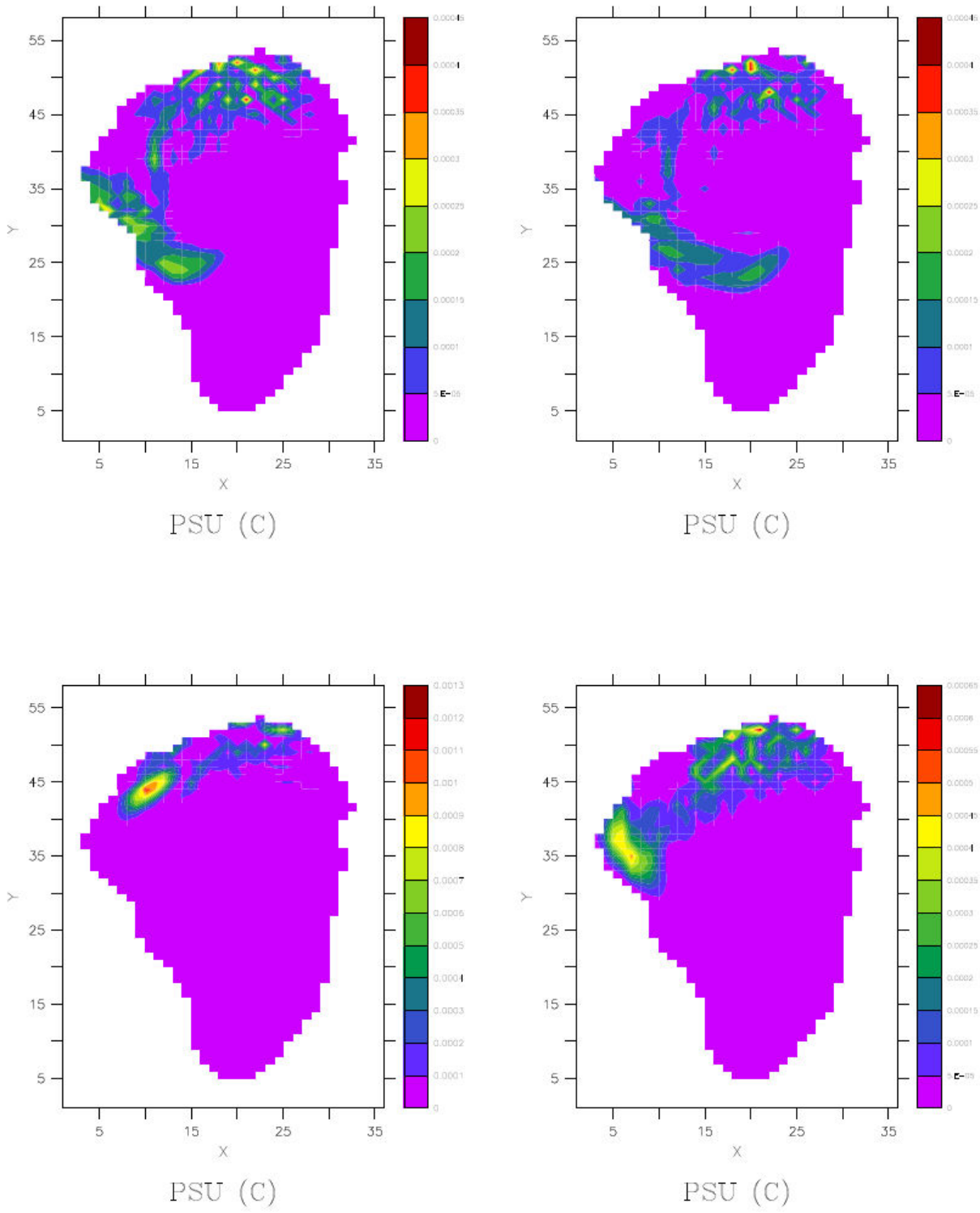

Figure 50: Tracer dispersion in the lake 96, 120, 144 and 168 hours after the tracer was introduced in its initial location at the Jordan River inflow.

Model summary
Limnological parameters (water currents, temperature vertical profile) were simulated using a hydrodynamical model. Comparisons of model results with observations showed reasonable agreement. The path of the Jordan River water was studied by introducing a short pulse of a passive tracer. Time snapshots of this tracer path (depth average) depict a cyclonic (anti-clockwise) propagation; the time scale in which the tracer advanced to the deep part of the lake was several days.

Data integration, interim conclusions and revised hypothesis

The bloom events of many dinoflagellates in fresh water and oceanic environments are characterized by a patchy distribution. Such heterogenic spatial distribution was reported for the spring bloom of the dinoflagellate *Peridinium gatunense* in Lake Kinneret (Pollingher 1988, Berman and Rohde 1971, Serruya and Berman 1975). More recently, satellite images clearly demonstrated that phenomenon (Yacobi and Schlichter 2004, Yacobi 2006). Processed satellite images presented in this report show the temporal dynamics of *Peridinum* patches in Lake Kinneret before, during and shortly after our study. The high areal resolution (300x300m) of the satellite data is the best snap shot we can obtain for the spatial distribution of chlorophyll in Lake Kinneret. This documentation can be done only once a day at the most, with high chances that atmospheric and wheather interferences will block the reception of a clear picture day after day. Thetrefore processed satellite images provide an excellent description of the system at a given time but are not enough when the system dynamics is questioned and orizontal migration rates of patches are at a time scale of hours. Only direct measurments that are done at a large number of sampling points and at an hourly rate (or at least several times a day) can provide the information required to describe the dynamics of the patchy phenomenon and for understanding the biological and physical processes affecting it.

There are two main operational questions related to the patchy phenomenon and the attempt to describe it and to follow its dynamics: 1. How to determine the patch dimensions? 2. What are the best ways to follow its migration and spatial and temporary dynamics?

How to determine the patch dimensions?

The spatial distribution of ecosystem variables such as chlorophyll or biomass concentration in a patch formation should follow a specific pattern in which a clear concentration gradient is measured from the patch boundaries to its central zone (Figure 27B). The concentration of biomass parameters as well as metabolic activities should increase as the patch central area is approached. A rather steep gradient is expected with one order of magnitude difference between the concentrations inside the patch and outside its boundary. The definition of the patch boundaries is rather operational, and for most of the cases covered in this study, chlorophyll concentration outside patches ranged between 25 and 100 $mg \cdot m^{-3}$ (Table 7). Inside a patch however, chlorophyll concentration ranged between 150 and 700 $mg \cdot m^{-3}$.

The horizontal dimensions of a patch vary; therefore the determination of a patch size is an operational issue, i.e. what is the resolution of the sampling grid. In a previous study (Sukenik et al., 2004) we determined the distribution of phytoplankton in Lake Kinneret based on vertical profiles measured in 24 sampling stations, evenly distributed in the lake (each sampling point roughly represents an area of 5 Km^2. In that study we observed at a certain day a definite large

patch of high chlorophyll concentration, assigned to a dense population of *Peridinium*, that was located at the center of the lake, with smaller patches of slightly lower chlorophyll levels located elsewhere. In the present study we repeatedly sampled a predefined area of 6 km^2 in the northern part of the lake. The sampling stations were distributed in that area to form a precise sampling grid that with 8 stations separated by 500 or 1500 m from each other (Figure 1). However due to the rapid dynamics and the apparent dimensions of *Peridinium* patches, only 30% of the sampling events represent in-patch data, whereas 70% of the sampling events were outside the patch (Table 7).

Table 7: Summary of sampling times and stations in accordance with their location inside or outside *Peridinium* patch, based on chlorophyll concentration.

	Date	Time	No of stations inside a patch (chl range -mg/m^3)	No of stations outside a patch (chl range -mg/m^3)
T1	March 26, 2007	1600 – 2045	2 (~150)	9 (50-100)
T2	March 26, 2007	2300 – 0130	4 (200)	7 (25-100)
T3	March 27	0400 – 0700	5 (150-200)	6 (25-100)
T4	March 27	1030 - 1400	5 (250-700)	6 (25-100)
T5	March 27	1630 - 1930	3 (250-400)	9 (50-100
T6	March 28	0000 - 0300	3 (~150)	9 (50-100)
T7	March 28	0800 - 1200	3 (200-300)	9 (25-100)
Total			25	52

The definition of patch dimensions and the evaluation of the dynamics of their migration require frequent sampling and near real time data acquisition. One option is to continuously follow the same patch its creation, evolution and dispersion. This approach requires long hours of continuous surveillance of the patch location and frequent sampling inside and outside the patch. The surveillance can be done by floating drogues assuming that the patch dynamics is mainly controlled by currents and waves. An alternative approach that was practiced in the current study was to define a priory a sampling grid of known dimensions and precise location. The location of the grid was chosen based on initial information collected at a larger area were *Peridinium* patches were observed. It is expected that under these conditions Peridinium patches will migrate across the sampling grid and the data collected during several consecutive sampling campaigns will represent inside and outside the patch conditions (Table 7). It is assumed that during the experiment period (ca 72 hrs) different patches migrated via the sampling grid, in some cases large portion of the patch were sampled whereas in other cases only the edges of a patch were sampled. Disadvantages of this approach are potential variability among patches; the sampled patches could be of different age or different geographic location and the high probability to repeated samples outside the patch relative to inside the patch.

Formation and migration of Peridinium patches.

It is generally accepted that physical forces and biological processes govern the formation of plankton patches in marine a lacustrine environments (Levine & Segel 1976, Donaghay &

Osborn 1997). Denman (1976) suggested that phytoplankton patch formation is less affected by physical process when growth rates are high, but dominated by physical processes, when growth rates are low. Taking into account that the location of the experiment was at a close vicinity to the Jordan River entrance to Lake Kinneret, a site which is characterized by a permanent supply of nutrients and other growth factors it is expected that the emerging *Peridinium* population will maintain high growth rate as long as its location is restricted to the Jordan River inlet area. The data presented in Figures 30 and 31 propose high correlation between the size of the *Peridinium* population (in terms of chlorophyll concentration) and the ratio of Jordan River water (traced by low salinity, low chloride and high nitrate concentrations) in the studied location. Satellite images (Figure 4) and earlier studies (Figure 1) indicate that the *Peridinium* patches exist mainly in the northern part of the lake where Jordan River enters the lake. Therefore we propose that area as the site of population development and growth. Such a growth is supported by nutrients and chemical conditions provided by the river inflow.

The distribution of the developing population is facilitated by the "track" of Jordan River stream in Lake Kinneret. In an ideal model it is perceived that a bulk of water enriched with *Peridinium* population is disintegrated from the "hatching" and "nursing" area (Jordan River inlet area) and starts its migration in the lake in accordance with the physical and hydrodynamic forces. The Peridinium population continues to take advantage of the relatively nutrient enriched confined pocket and use it for further duplications. It is important to note that *Peridinium* duplication can be maintained for one or tow divisions even when the nutrient diminished due to its wide range of nutrient yields. The patch migration continues along the "Jordan River" trail in Lake Kinneret, from the north area, the site of the population emergence, along the northwest cost and to the lake center (Figure 51), in accordance with the simulations presented in Figures 49 and 50 for the dispersion of an inert tracer in Lake Kinneret. Since the *Peridinium* patch is definitely not an inert tracer, its signal increases during the migration process. Based on this model it is expected that a single patch migrating in the lake is of different age or developmental stage then another patch. Furthermore, a migrating patch can be a source of additional secondary patch which can be disintegrated from the main patch due to temporary wind gusts and local currents. Such an event is most likely to occur as the *Peridinium* population is concentrated as a thin layer at the upper part of the water column, a daily phenomenon associated with the well reported phenomenon of diurnal vertical migration - DVM (Figures 7 and 9 and Pollingher 1988).

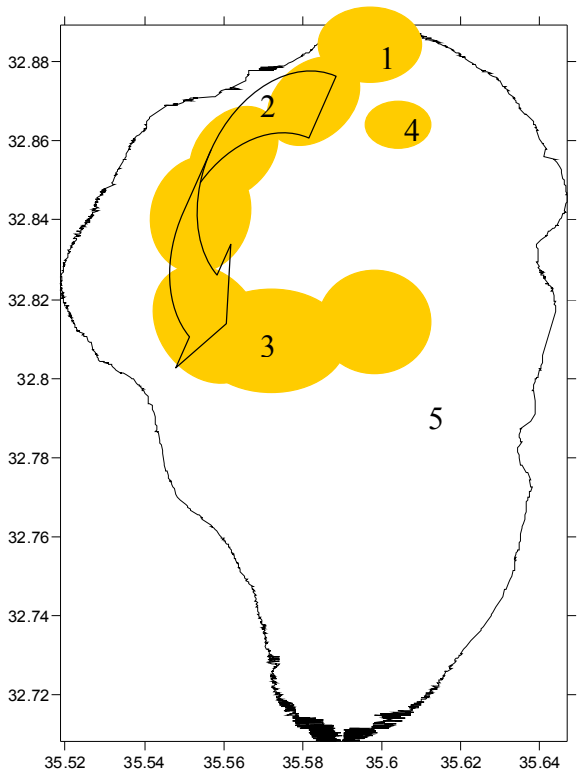

Figure 51: Schematic presentation of model postulating the patchy nature of Peridinium bloom in Lake Kinneret. 1) The bloom is initiated in the northern area, where River Jordan, that carries nutrients of winter floods, enters the lake. 2) Flood events carry water mass in the lake in a well defined track. 3) The *Peridinium* cells maintain their location within the plume of River Jordan waters and perform one or more cellular divisions. 4) Wind gusts cause the formation of secondary patches which are disintegrated from the main patch. 5) The *Peridinium* population in the migrating patch is aged due to lack of nutrients (mainly CO_2), exposed to high temperatures and pH and doomed to death

While the postulated model provide general explanations and processes for the formation and migration of *Peridinium* patches, many related questions and observations were left unresolved:

- What are the physiological and cellular mechanisms that help the cells to maintain their location within the patch, and keep the bulk of the population within a relatively confined volume?
- How the population maintains its patchy structure for a long period during which it migrates to the central areas of the lake and as far as the southern part of the lake?
- Are the physiological properties of the *Peridinium* population in one patch different from those of a near by or remotely separated other patches?
- Is the population of a given patch is genetically homogenous? Can we determine genetic variations in *Peridinium* populations that inhibit patches at different locations (south vs north)?
- Why the patchy phenomenon is restricted to *Peridinium* (or other dinoflagellate) population and is not observed with other phytoplankton populations that bloom in Lake Kinneret?

References

Berman T. and Rodhe W. 1971. Distribution and migration of *Peridinum* in Lake Kinneret. Int. Ver. Fur theor. Und angewa. Limnologie. 19: 266-276.

Brocchini, M., M.G. Wurtele, G. Umgiesser and S. Zecchetto 1995. Calculation of a Mass-Consistent Two-Dimensional Wind Field with Divergence Control. Journal of Applied Meteorology, 34 (11): 2543-2555.

Cressman G. P., 1959. An operational objective analysis system. Mon. Wea. Rev., 87: 367-374.

Hambright, K.D., Zohary, T. and Gude, H., 2007. Microzooplankton dominate carbon flow and nutrient cycling in a warm subtropical freshwater lake. Limnol. Oceanog., 52:1018–1025.

Large, W. G., J. C. Mcwilliams, and S. C. Doney. 1994. Oceanic vertical mixing: A review and a model with a nonlocal boundary layer parameterization. Rev. Geophys. 32: 363-403.

Mellor, G.L., and T. Yamada. 1982. Development of a turbulence closure model for geophysical fluid problems. Rev. Geophys. Space Phys. 20: 851-875.

Ostrovsky, I. and Sukenik, A. 2008. Spatial heterogeneity of biogeochemical parameters in a subtropical lake. *In Monitoring and Modeling Lakes and Coastal Environments (P. K. Mohanty, ed.)*. Springer, 248 p.

Pollingher, U. 1988. Freshwater armored dinoflagellates: growth, reproductive strategies and population dynamics. In: Sandgren, C. (ed.), *Growth and Reproduction Strategies of Freshwater Phytoplankton*. pp. 134-174.Cambridge University Press.

Rimmer A., Y. Aota, M. Kumagai and W. Eckert, 2005. Chemical stratification in thermally stratified lakes: A chloride mass balance model. Limnol. Oceanogr. 50: 147-157.

Serruya.C and Berman T. 1975. Phosphorus, nitrogen and the growth of algae in Lake Kinneret. J. Phycol. 11: 155-162.

Shilo E, Y. Ashkenazy, A. Rimmer, S. Assouline, and Y. Mahrer. 2007. The effect of wind variability on topographic waves: Lake Kinneret case. (Journal of Geophysical Research – Oceans, in press).

Song, Y., and D. B. Haidvogel. 1994. A semi-implicit ocean circulation model using a generalized topography-following coordinate system. J. Comp. Phys. 115: 228-244.

Sukenik, A., Yacobiy, Y.Z., Wynne, D. And Parparov R. 2004. Physiological variability within *Peridinium gatunense* (Dinoflagellate) population during its patchy bloom in Lake Kinneret. Verh. Internet. Verein. Limnol. 29: 365-368.

Wynne, D., Patni, N.J., Aaronson, S., Berman, T., 1982. The relationship between nutrient status and chemical composition of *Peridinium cinctum* during the bloom in Lake Kinneret. Journal of Plankton Research 4, 125-136.

Yacobi, Y.Z., and Schlichter, M. 2004. GIS application for mapping of phytoplankton using a multi-channel fluorescence probe derived information. *In*: (Yangbo Chen, Kaoru Takara, Ian D. Cluckie & F. Hilaire De Smedt, eds), GIS and Remote Sensing in Hydrology, Water Resources and Environment, IHAS Publication 289: 301-307, International Association of Hydrological Sciences Press, Wallinford, UK

Yacobi Y. Z. 2006. Temporal and vertical variation of chlorophyll a concentration, phytoplankton photosynthetic activity and light attenuation in Lake Kinneret: possibilities and limitations for simulation by remote sensing. J. Plankton Res. 28: 725 - 736.

Zohary, T. and Makler V. 2004. Phytoplankton parameter values In: Final report – Physiological Experiments, Lake Kinneret Water Quality Management and Optimization Support System-Phase 2. T. Zohary Ed. Kinneret Limnologcal Laboratory.

Zohary, T., Pollingher, U., Hadas O. and Hambright, K.D. 1998. Bloom dynamics and sedimentation of *Peridinium gatunense* in Lake Kinneret. *Limnol. Oceanogr*. 43: 175-186.